Bioorganic & Medicinal Chemistry 22 (2014) 4135–4150

Contents lists available at ScienceDirect

Bioorganic & Medicinal Chemistry

journal homepage: www.elsevier.com/locate/bmc

Fragment-based hit discovery and structure-based optimization of aminotriazoloquinazolines as novel Hsp90 inhibitors

Elena Casale *, Nadia Amboldi, Maria Gabriella Brasca, Dannica Caronni, Nicoletta Colombo, Claudio Dalvit †, Eduard R. Felder, Gianpaolo Fogliatto, Arturo Galvani, Antonella Isacchi, Paolo Polucci, Laura Riceputi, Francesco Sola, Carlo Visco, Fabio Zuccotto ‡, Francesco Casuscelli *

Oncology, Nerviano Medical Sciences, Viale Pasteur 10, 20014 Nerviano (MI), Italy

ARTICLE INFO

Article history:
Received 9 April 2014
Revised 21 May 2014
Accepted 23 May 2014
Available online 14 June 2014

Keywords:
Fragment based hit discovery
FAXS-NMR screening
Structure-based design
Hsp90 inhibitors
Anti-cancer agents

ABSTRACT

In the last decade the heat shock protein 90 (Hsp90) has emerged as a major therapeutic target and many efforts have been dedicated to the discovery of Hsp90 inhibitors as new potent anticancer agents. Here we report the identification of a novel class of Hsp90 inhibitors by means of a biophysical FAXS-NMR based screening of a library of fragments. The use of X-ray structure information combined with modeling studies enabled the fragment evolution of the initial triazoloquinazoline hit to a class of compounds with nanomolar potency and drug-like properties suited for further lead optimization.

1. Introduction

Heat shock protein (Hsp90) is a molecular chaperone that plays a role in the conformational stability, maturation, and function of several proteins, including many oncogenic kinases, whose dysfunctional activation has been collectively described as constituting the hallmark traits of cancer.[1] Hsp90 inhibitors cause the destabilization and degradation of more than a hundred Hsp90 client proteins,[2] and showed promising antitumor activity in several preclinical model systems.[1c] For these reasons, Hsp90 emerged in the last decade as a major therapeutic target and a great deal of efforts have been dedicated to the discovery of new inhibitors[3] and some of them are currently tested in clinical trials.[4]

Fragment Based Drug Discovery (FBDD) is an established approach for lead discovery and has been successfully applied in drug research programs,[5] with a number of examples concerning the optimization of Hsp90 inhibitors.[6] A high-quality fragment library together with valid biophysical techniques for screening, assisted by crystallography, provide remarkable scope in support of the medicinal chemistry elaboration of fragment hits into leads. Screening of a relatively small number of low molecular weight fragments can efficiently sample the relevant chemical space, even though fragments generally have low binding affinities for the intended target. Hence, the choice of sensitive and robust biophysical methods able to detect weak binders is crucial.[7,8] Here, among the many methods for detecting the fragment binding, the FAXS (Fluorine chemical shift Anisotropy and eXchange for Screening) competition assay, which utilizes the favorable properties of Fluorine NMR spectroscopy,[9] was chosen for Hsp90 fragment screening. In our experience this method has proven to be a powerful approach since it combines sensitivity, efficiency, reliability and throughput while minimizing protein consumption. Furthermore, it provides straightforward evidence of a molecule's biophysical effects on the targeted binding site of a protein, helping to distinguish general unspecific binders.

In the present work we report on the fragment-based approach for the identification of aminotriazoloquinazoline as an original chemotype in the context of Hsp90 inhibition efforts, attractive for its potential to introduce chemical novelty. Although the triazoloquinazoline scaffold has been previously utilised a.o. in adenosine receptor antagonists,[10] for the treatment of disorders mediated by purine receptors,[11] and also in phosphodiesterase PDE10A inhibitors,[12] our 2-amino-5-alkyl-[1,2,4]triazolo[1,5-*a*]quinazoline subtype was not described so far. We therefore

* Corresponding authors. Tel.: +39 0331 581041; fax: +39 0331 581347 (E.C.); tel.: +39 0331 581326; fax: +39 0331 581347 (F.C.).
E-mail addresses: elena.casale@nervianoms.com (E. Casale), francesco.casuscelli@nervianoms.com (F. Casuscelli).
† Current address: University of Neuchatel, Avenue de Bellevaux 51, 2000 Neuchatel CH, Switzerland.
‡ Current address: University of Dundee, Dow Street, Dundee DD1 5EH, Scotland, UK.

http://dx.doi.org/10.1016/j.bmc.2014.05.056
0968-0896/

prioritized the optimization of this fragment, whose structure-guided evolution led us to obtain nanomolar inhibitors of Hsp90 in just a few cycles of chemical modification and biological testing. An alternative binding mode of optimized intermediates was revealed by crystallographic studies and offered an additional path for the medicinal chemistry expansion and further evolution of this attractive chemical class.

2. Design and synthesis

2.1. NMR screening and hit identification

In search of novel chemical entities as Hsp90 inhibitors we engaged in a fragment-based approach, which included the screening of an internal library of fragments followed by an extensive structure-guided design phase supporting inhibitor evolution to improve potency and drug-like properties of the initial hits.

A library of approximately 1200 fully characterized fragment-like molecules including commercial compounds, proprietary building blocks and advanced intermediates from medicinal chemistry programs was assembled. Our definition of the fragments chemical space is based on the following parameters: MW (Molecular Weight) <300 Da, (variable if halogen or sulfur atoms are present), PSA (Polar Surface Area) $\leqslant$ 80 Å^2, *c*log*P* <3, number of rotatable bonds <4, total number of H-bond acceptors/donors between 3 and 6.[13] We also consider fragments with asymmetric centers and sp^3-carbon rich molecules, which might be advantageous in exploring demanding biological targets.[14] The resulting library of fragments was then subjected to chemoinformatic filters to ensure the absence of undesirable chemical functionalities, and screened with the SPAM (Solubility, Purity and Aggregation of the Molecule)[15] filter approach for the exclusion of aggregation or low kinetic solubility as potential alert of PAINS[16] (promiscuous or pan-assay interference compounds) frequently encountered during primary screening.

A subset of this library including about 300 fluorinated fragments (CF or CF_3 containing molecules),[9c] was first screened against the *N*-terminal domain of human Hsp90α for the identification of a binder to be used as a probe ('spy molecule') in the FAXS NMR experiment. The two fluorinated binders **1** and **2**, belonging to the frequently described aminopyrimidine chemical motif and structurally similar to the derivative found in the PDB structure 2XHR, were identified (Fig. 1).[17] These inhibitors showed a competitive behavior with respect to ATP with a binding affinity constant (K_i) of 29.6 μM and 7.5 μM for **1** and **2**, respectively, as measured in a Fluorescence Polarization (FP) assay. Compound **2** having the benzodioxolane group was deemed to be a better probe for the identification of ATP binding site ligands, as well as alternative site binders, and thus it was selected as the spy molecule. Despite its low solubility (~15 μM) was easily identified in the ^{19}F NMR direct binding assay and performed well as spy molecule in the ^{19}F NMR competition binding assay and in the K_i measurements of the identified hits and synthesized molecules.

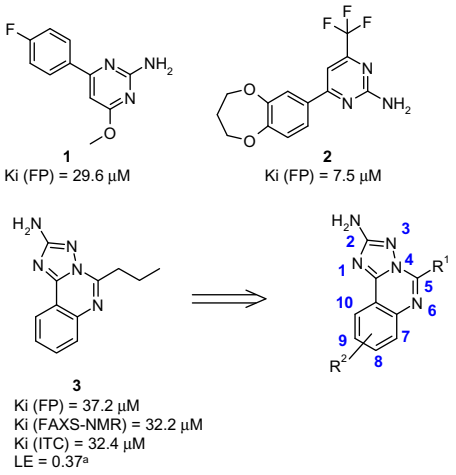

Figure 1. Spy molecules **1** and **2**, fragment hit **3** and the 2-aminotriazoloquinazoline core structure.

Mixtures consisting of ten fragments were screened with the FAXS NMR displacement assay, using 6 μM of the spy molecule **2** and 0.6 μM of the catalytic domain of Hsp90α, as described in the Section 5 (see also the Supporting information Fig. Si 1).

A straightforward mixture deconvolution process identified 23 ligands (hit rate of 1.9%). The hits progressed to crystallization trials and structural data were obtained for four compounds. The discovery and optimization of one of these fragments belonging to the resorcinol class of small molecule inhibitors of Hsp90, has already been reported.[18] In a complementary effort we pursued also the development of a novel ATP competitive inhibitor with a distinct chemotype. To this end the aminotriazoloquinazoline hit **3** (Fig. 1) was selected for full characterization and chemical optimization. FAXS NMR titration measurement of **3** was performed and a K_i of 32.2 μM was calculated corresponding to a ligand efficiency (LE) of 0.37 which was considered good[19] and suited for the further exploration of the fragment class. The binding affinity to Hsp90 was also confirmed by isothermal titration calorimetry (ITC) experiments (see Supporting information Fig. Si 2) and FP assays reporting a K_i of 32.4 μM and 37.2 μM, respectively. The structures of the fluorinated binders **1** and **2** and fragment **3** with the corresponding Hsp90 K_i values and the ligand efficiency (LE) are reported in Figure 1.

To facilitate the chemical expansion, the crystal structure of compound **3** bound to the ATPase domain (aa 9-236) of Hsp90α (Fig. 2) was determined. Interestingly, compound **3** does not occupy the adenine binding site, rather it is located in an adjacent induced-fit pocket by triggering a rearrangement of residues 103–111, which in the presence of the ligand adopt a helical conformation. This second binding site has been documented previously and compounds with similar behavior have been

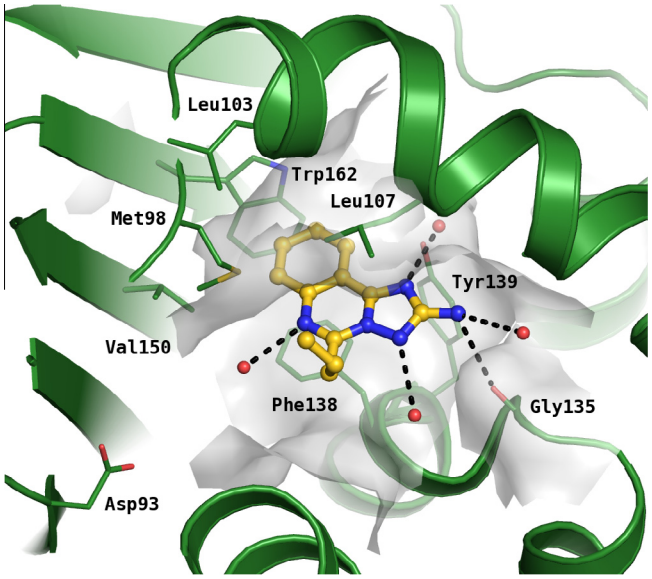

Figure 2. X-ray structure of the initial fragment hit bound to the N-terminal domain of Hsp90. Compound **3** (yellow carbon atoms) and key residues of the active site (green carbon atoms) are shown. The grey surface represents the induced pocket, while ordered water molecules are shown as red spheres and hydrogen bonds as black dashed lines.

reported.[20] These conformational changes do not modify the adenine binding site, preserving the positions of the key residue Asp93 and thus offering opportunities for the design of new inhibitors taking advantage of additional interactions with the enzyme.

Compound **3** binds deep inside the lipophilic pocket, with its propyl chain pointing out toward the ATP sugar region. The interactions of the ligand with the protein are mainly hydrophobic. The triazoloquinazoline core is stacked between the side chain of Leu107 and Phe138 making a (face-to-face) π–π stacking with Phe138 and an additional face-to-edge π-stacking contact with Trp162.[20,21] Other favorable hydrophobic contacts occur with Met98, Leu103, Tyr139, Val150, whilst the polar interactions are only weak hydrogen bonds between the amino group and the backbone carbonyl group of Gly135 and a conserved water molecule. Additional hydrogen bonds are found between the nitrogen atoms of the scaffold (N1, N3 and N6) and three conserved water molecules (Fig. 2).

Amino-triazoloquinazoline **3** offered an attractive starting point for structure-based optimization mainly due to the good ligand efficiency, the chemical feasibility and the peculiar binding mode in the alternative binding site. Furthermore, the replacement of the propyl chain with well known structural motifs (i.e., resorcinol, aminopyrimidine)[5] was expected to provide opportunities to explore the adenine-binding region.

2.2. Chemistry

Scheme 1 illustrates the aminotriazoloquinazoline synthesis route with R^1 diversification and variations of the R^2 substituents on the benzene ring of the scaffold (**7a**–**v**).[22] As previously reported, the aminotriazoloquinazoline core structure can be obtained from a key benzoxazinone intermediate upon reaction with aminoguanidine bicarbonate, in pyridine, at reflux or by microwave assisted heating.[12,23]

A direct conversion of anthranilic acids **4a**–**d** into benzoxazinone **6a**–**d** was performed upon treatment with neat butyric anhydride. Alternatively, starting from anthranilic acids **4e**–**v** the access to the amide derivatives **5e**–**v** was accomplished by reaction with the suitable acyl chlorides under microwave heating conditions.

The acylated anthranilic acids **5e**–**v** were precipitated with HCl, filtered, and used without further purification. Access to the key benzoxazinone derivatives **6e**–**v** was achieved upon treatment of **5e**–**v** with acetic anhydride at reflux for 5 min. The final products **7a**–**v** were then obtained by reacting benzoxazinones **6a**–**v** with aminoguanidine in the presence of pyridine. Compounds conveniently precipitated slowly in pure form from the reaction mixture. The overall yields ranged from 10% to 50%, and the synthetic sequence tolerated a broad variety of substitutions. Decoration and modification of the core structure were performed following

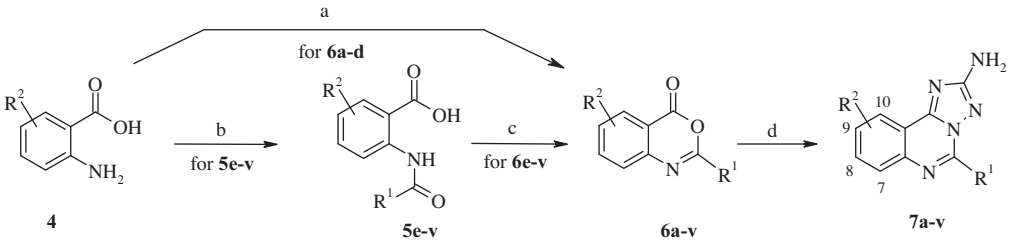

Cpd	R^1	R^2	Cpd	R^1	R^2
7a	n-Pr	7-OMe	**7k**	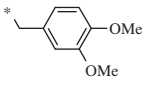	H
7b	n-Pr	10-F			
7c	n-Pr	7-Me	**7l**	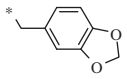	H
7d	n-Pr	7-Cl			
7e	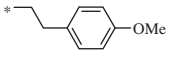	H	**7m**	"	8-F
			7n	"	8-SO_2NH_2
7f	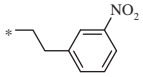	H	**7o**	"	10-F
7g	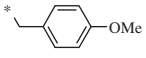	H	**7p**	"	8,10-F
			7q	"	10-Cl
7h	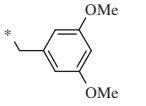	H	**7r**	"	7-OPMB
			7s	"	8-OPMB
7i	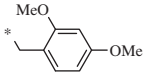	H	**7t**	"	9-CN
			7u	"	8-NO_2
7j	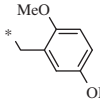	H	**7v**	"	8-COOH

Scheme 1. Synthesis of aminotriazoloquinazolines **7a**–**v**. Reagents and conditions: (a) Butyric anhydride, 160 °C, microwave, 10 min; (b) acyl chlorides R^1COCl, pyridine, DCM, 120 °C, microwave, 5 min; (c) acetic anhydride, 130 °C, 10 min; (d) aminoguanidine bicarbonate, pyridine, 180 °C, microwave, 20 min.

suitable functional group transformations, as reported in Scheme 2. Boron tribromide mediated deprotection of methoxy compounds **7e**, **7h**, and **7i** gave corresponding phenols **8a–c**. Instead, the 8-hydroxyl derivative **9a** and **9b** were obtained after cleavage of the PMB protecting group by treatment with HCl. The nitro group of **7f** and **7u** was transformed into the amino group delivering compounds **10a–b** by standard hydrogenation. Compound **11** was successfully prepared from the corresponding nitrile **7t** upon treatment with borohydride/cobalt chloride. Halogenated derivatives such as 7- or 8-bromo intermediates were considered good synthons for expansion but unfortunately neither Suzuki nor Buchwald reactions worked. Moreover, installation of a solubilizing tether via reductive amination performed on compound **10b** failed.

Conversely, introduction of such groups were successfully achieved by nucleophilic aromatic substitution[24] on the 8- and 10-fluoro derivatives **7m** and **7o** yielding the desired compounds with a nitrogen containing moiety **12a–g** and. The amide preparation following path f (Scheme 2) was performed by activation of the carboxylic acid intermediate **7v** with TBTU in the presence of the selected amines delivering the desired compound **13a–b** in fair yields. Since the evaluation of R^2 substituents in 8 or 10 position afforded products with good potency and improved solubility, the syntheses of di-substituted derivatives with the best groups in position 8 and 10 were attempted.

As shown in Scheme 3, the intermediate **5p** (prepared as reported in Scheme 1) was reacted with trimethylsilyldiazomethane to afford the 2-(2-benzo[1,3]dioxol-5-yl-acetylamino)-4,6-difluoro-benzoic acid methyl ester that upon treatment with a suitable amine such as *N*-methylpiperazine in DMSO at 80 °C afforded selectively the 4-(4-methylpiperazinyl)-6-F derivative **15** via the 4-fluorine replacement, likely due to the bulky amine's steric effect. After ester hydrolysis, the acid was condensed via benzoxazinone **16** to the aminotriazoloquinazoline **17** in a similar manner to that previously described.

Regrettably the attempts to expand the reaction with additional amines proved to be limiting since the reaction with primary amines in similar conditions gave an unresolved mixture of regioisomers via the 4-fluoro or 6-fluoro replacement, also when a more steric hindered ester was evaluated.

Alternatively, the introduction of solubilizing groups was successfully achieved by nucleophilic aromatic substitution on 8,10-difluoro-2-aminotriazoloquinazoline derivative **7p**, obtained from intermediate **5p** as previously described, delivering compounds **18a–e** as reported in Scheme 3.[24] However, the aromatic nucleophilic substitution did not derivatize the 8-position, whereas the 10-fluorine group resulted to be more reactive and underwent the replacement, although preventing a bis substitution (Scheme 3).[24]

3. Results and discussion

The aminotriazoloquinazoline fragment **3** being commercially available, additional structural analogues were searched in databases from vendors. Twenty additional derivatives were then purchased and tested in the FAXS NMR binding assay, but only modest Hsp90 inhibition was measured. Initial medicinal chemistry efforts were focused on the Fragment growing approach.[17a,25] To this purpose, a left-hand substitution exploration was performed with small R^2 substituents on the phenyl ring, resulting

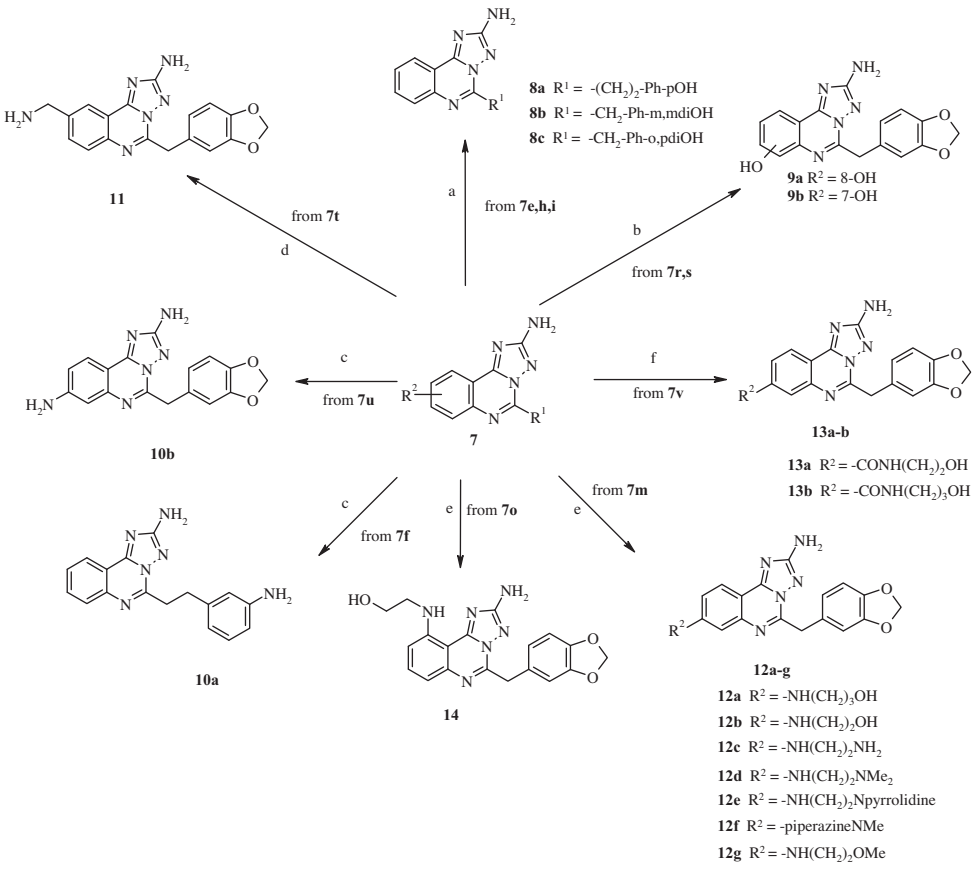

Scheme 2. Synthesis of aminotriazoloquinazoline derivatives. Reagents and conditions: (a) 1 M BBr_3 in DCM, rt, 120 h; (b) HCl 4 M dioxane, rt 18 h; (c) cyclohexene, 10% Pd/C, MeOH, 65 °C, 2 h; (d) $NaBH_4$, $CoCl_2 \times 12\ H_2O$, THF/MeOH, rt, 18 h; (e) amines, 140 °C, 2–8 h; (f) amines, TBTU, DiPEA, DCM, rt, 4 h.

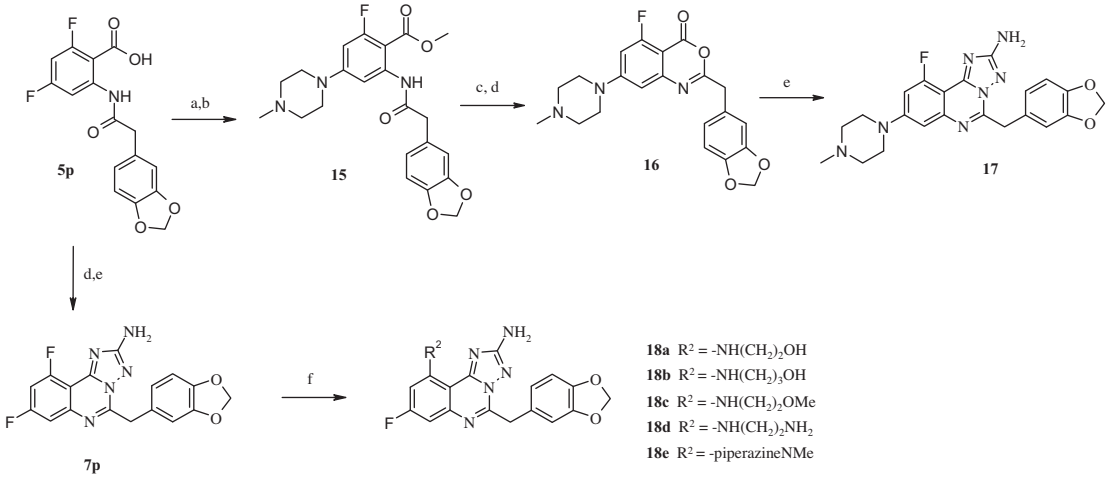

Scheme 3. Synthesis of 8–10 di-substituted aminotriazoloquinazoline derivatives. Reagents and conditions: (a) TMS-CHN_2, MeOH, DCM, rt, 1 h; (b) *N*-methylpiperazine, DMSO, 80 °C, 2 h; (c) LiOH, THF/MeO/H_2O (7:2:1) rt, 18 h; (d) acetic anhydride, 130 °C, 10 min; (e) aminoguanidine bicarbonate, pyridine, 180 °C, microwave, 20 min; (f) amines, 140 °C, 2–8 h.

Table 1
Optimization iteration: biochemical potency, ligand efficiency and solubility

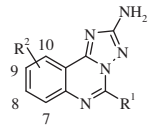

Compd	R^1	R^2	K_i[a] (μM)	LE[b]	Sol[c]
3	*n*-Pr	H	32.2	0.37	70
7a	"	7-OMe	22.7	0.34	30
7b	"	10-F	28.6	0.35	86
7c	"	7-Me	16.7	0.37	10
7d	"	7-Cl	23.4	0.36	30
7e	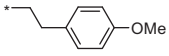	H	NE[d]		3
8a	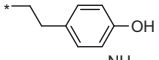	H	NE[d]		3
10a	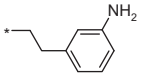	H	15.2	0.28	12

[a] K_i were obtained with FAXS NMR and values are an average of two or more determinations.
[b] Ligand efficiency LE = $-1.4\log(K_i)$/HAC; HAC = heavy atom count.[19]
[c] Kinetic solubility PBS pH 7.4 μM.
[d] No effect.

in the structure–activity relationship (SAR) presented in Table 1. The analogues **7a**–**d** containing minimal structural modifications gave some activity improvement.

On the other hand, the co-crystal structure of **3** in Hsp90 (Fig. 2) indicates that the propyl chain points to a solvent exposed area towards a cluster of H bond accepting groups (Asn51, Ser52, Asp54) interacting with a conserved water molecule. Therefore, a possible development of **3** could extend a hydrophilic head from the propyl group to target the above mentioned interactions. Compound **8a** and **10a** were designed to assess this structure-based hypothesis (Table 1). While **10a** provided a modest enhancement of the affinity, the phenolic derivative **8a** was inactive, possibly because its solubility was very low.

Additionally, we developed a fragment linking strategy with the help of a large amount of structural information publicly available.[17a,25] In particular, the overlay of the crystal structures of radicicol analogues or resorcinol compounds (PDB 2IWU, 2BT0 and 2UWD) highlighted the possibility to extend the initial fragment to access the adenine region. Therefore, linking of aminotriazoloquinazoline with the well known resorcinol moiety was considered an option to develop new derivatives likely to establish interactions with the key residue Asp93.[17,25] Modeling studies indicated the position 5 of the triazoloquinazoline core as the best one to connect our fragment to the resorcinol moiety using a flexible –CH_2– linker. The in silico analysis also highlighted how either the *ortho*–*para* or the *meta*–*meta* resorcinol regioisomers could reproduce the favorable network of interactions. Following this approach, compounds with an aryl group bearing two hydroxyls were synthesized according to Schemes 1 and 2. Incorporation of dihydroxyphenyl moieties tethered to C-5 of the scaffold with a –CH_2– linker was performed leading to the compounds **8b** and **8c** (Table 2) that showed a fivefold improvement of affinity. The co-crystal structure of **8b** in complex with Hsp90 confirmed molecular modeling suggestions (Fig. 3A). As expected, the dihydroxyphenyl ring of **8b** occupies the adenine site with a binding mode reminiscent of other resorcinol containing compounds.[26,27] The key hydrogen bond interaction between the carboxylate side chain of Asp93 and one of the two hydroxyl groups is conserved. In addition the two hydroxyl groups form a network of water mediated interactions with the neighboring residues Gly97, Ser52 and Leu48. The recognition of the resorcinol moiety seems to be the 'driving force' of the binding and induces changes in the orientation of the aminotriazoloquinazoline moiety that adopts a slightly different orientation compared to the initial hit **3** (Fig. 2), although it is still accommodated in the hydrophobic pocket.

Intriguingly, compounds **7h** and **7i**, synthetic intermediates of **8b** and **8c**, resulted even more active. Taking into consideration the binding mode of **8b** it was not trivial to explain the activity of **7h** and its analogue as the two molecules lack the hydroxyl groups that are essential for the interactions with Asp93 and the conserved water molecules. Thus, the structure of compound **7h** in complex with Hsp90 was solved (Fig. 3B). It turns out that compound **7h** binds in a completely different manner compared to his hydroxyl analogue **8b** (Fig. 3A). The molecule flips so that the aminotriazoloquinazoline group occupies the adenine pocket and its amino group forms the key hydrogen bond to the side chain of Asp93. The additional interactions with the protein residues are water mediated: the three nitrogen atoms in position 2, 3, and 6 of the triazoloquinazoline core are bridged by several water molecules with the side chain of Asp93, Thr184 and Asn51, the

Table 2
Optimization iteration: biochemical potency, ligand efficiency and solubility of compounds **3**, **7f–k**, and **8b–c**

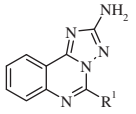

Compd	R^1	K_i[a] (μM)	LE[b]	Sol[c] (μM)
3	*n*-Pr	32.2	0.37	70
7g	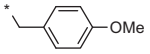	3.5	0.33	3
7h	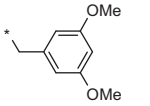	2.6	0.31	4
7i	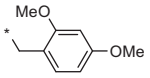	3.1	0.31	11
7j	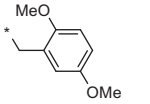	2.1	0.32	4
7k	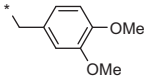	2.4	0.31	4
7l	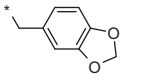	0.170[d]	0.39	15
8b	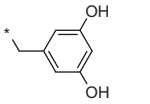	6.1	0.32	15
8c	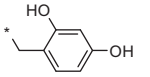	8.4	0.31	30

[a] K_i were obtained with FAXS NMR and values are an average of two or more determinations.
[b] Ligand efficiency LE = $-1.4\log(K_i)$/HAC; HAC = heavy atom count.
[c] Kinetic solubility PBS pH 7.4 μM.
[d] FAXS NMR assay detection limit.

backbone nitrogen of Gly97 and the backbone oxygen of Leu48 and Ile91. The 3,5-dimethoxyphenyl moiety occupies the induced pocket and is stacked between the side chain of Leu107 and Phe138, overlapping well with the triazoloquinazoline core space of compound **3**. This binding mode is reminiscent of the one described for the purine based inhibitor PU3.[20,28,29] The phenomena of fragment adopting different binding conformation, are well known during optimization of Hsp90 inhibitors as previously shown by others.[17a,25,30]

This binding mode switch was unexpected and in light of these results we could not exclude that the initial fragment **3** may bind to the protein in two different ways: either in the adenine pocket or in the hydrophobic site and that the crystallographic structure just trapped only one of them. The identification of these two binding modes was a breakthrough that yielded the opportunity to develop two different series starting from the initial hit. The potency and ligand efficiency, as well as novelty and diversity, encouraged us to prioritize compound **7h** for further explorations.

Optimization of **7h** initially focused on exploring the SAR of the substituent at position 5, taking inspiration from the already disclosed SAR developed for the optimization of the purine scaffold inhibitors.[28,29] Substituents on the aryl ring of this set of analogues allowed probing of potential protein interactions with the helical-conformation side chains of Phe138, Tyr139 and Trp162.

Activity data concerning analogues of **7h** are summarized in Table 2. The compounds with 4-methoxy and either a (2′–4′) or (3′–4′) or (2′–5′) di-methoxy benzyl group (**7g**, **7i–k**) were confirmed possessing good inhibitory activity comparable to **7h**, these groups being buried in a very hydrophobic cavity and making (as observed for **7h** in Fig. 3B) predominantly face to face π-stacking interactions with Phe138. Moreover, the methoxy group in 3′ (as deduced from Fig. 3B) is in place and distance to make a weak interaction with the hydroxyl group of Tyr139 that could explain the small difference in potency of **7h**, **7j** and **7k** compared to **7g** and **7i**. Additionally, the *ortho* substitution revealed a negligible effect on the binding (**7g** vs **7i** or **7h** vs **7j**). Introduction of the five membered dioxolane ring in 2′,3″ of the phenyl moiety led to **7l**, resulting in the most potent compound of the series. It showed a K_i of 0.170 μM with high ligand efficiency (0.39) and a 200-fold improvement in activity with respect to the original hit, (inhibitory potency approaching the limit of detection in FAXS assay). All the other analogues bearing either variously substituted phenyl groups or larger diphenyl systems did not show significant improvement in binding affinity (data not shown). Further substitutions on the benzodioxole moiety previously reported to be beneficial[25] led to inactive compounds likely due to the poor solubility (data not shown). Structure studies of **7l** confirmed the binding mode of

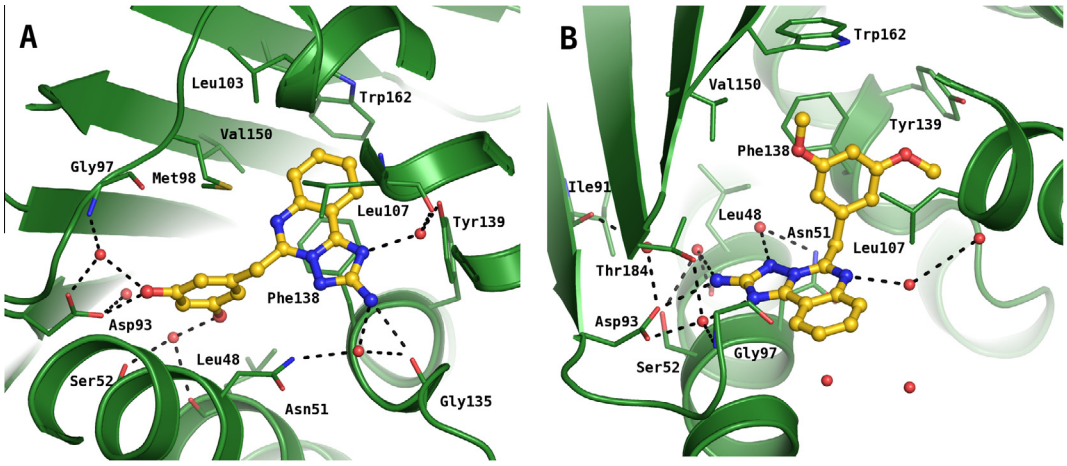

Figure 3. (A) View of compound **8b** bound in the active site of Hsp90. Compound **8b** (yellow carbons atoms) and key residues of the active site(green carbon atoms) are shown as sticks, ordered water molecules are shown as red spheres and hydrogen bonds as black dashed lines. (B) View of compound **7h** bound in the active site of Hsp90 **7h** (yellow carbons atoms) and key residues of the active site (green carbon atoms) are shown as sticks, ordered water molecules are shown as red spheres and hydrogen bonds as black dashed lines.

the parent compound **7h**. Interestingly the benzodioxole moiety occupies the pocket in a manner similar to the PU-DZ8 purines,[28,29] perfectly 'sandwiched' in the hydrophobic pocket with a water mediated interaction involving Tyr139 and Trp162 (See Supporting information Fig. SI 3).[31]

After the initial optimization process, the binding affinities of the new compounds reached the limits of sensitivity of the FAXS assay, therefore activity evaluation and SAR were assessed by Fluorescence Polarization (FP). Compound **7l** was tested in both FAXS NMR and Fluorescence Polarization (FP) assays and the K_i values observed were 0.170 μM and 0.035 μM, respectively (Table 3).

With the benzodioxole moiety identified as the best substituent for position 5, the next step of the optimization process focused on the exploration of positions 7–10 by the introduction of polar moieties aiming to improve both activity and solubility (Table 3), the latter representing a major concern and possibly a cause of the modest cellular activity measured. Towards this end, compound **11**, which contains an amino-methyl moiety attached on C-9, was prepared and tested. Unfortunately we observed a decrease in the activity likely due to steric repulsion. On the contrary, the insertion of a fluorine atom in position 10 led to the most potent compound (**7o**) with the highest ligand efficiency (0.46 kcal *per* heavy atom), even though position 10 is exposed to a severely hindered environment by the presence of residues Ile96 and Gly97. A 3-D structural insight of this compound (see Supporting information Fig. SI 4) revealed that the fluorine atom occupies a small pocket defined by residues Ile96 and Gly97, interacts with the carbonyl group of Gly97 and contributes to the anchorage with Asp93 through a water bridge network. Residues Ile96 and Gly97 restrain the shape and size of this pocket, so that only very small C-10 groups could be tolerated, as indicated by the lack of activity observed with the 10-chloro derivative **7q**.

Careful inspection of the crystal structure of **7l** revealed that the 7 and 8-positions of the triazoloquinazoline core point toward the solvent and are more suitable for the insertion of a variety of substituents for the improvement of potency and adjustment of physicochemical properties. Modeling studies suggested that we could gain additional potency by designing analogues that extend into the solvent exposed ribose binding pocket interacting with the side chains of Asp102 and Lys58. Surprisingly, the introduction of either an amino group or a hydroxyl group in position 8 (**10b** and **9a**, respectively) as well as a hydroxyl group on C-7 (**9b**) produced a marginally negative effect compared to **7l**. However, these groups are better tolerated than halogen, such as for **7m**, likely as a consequence of the electronic effect on the aromatic ring.

A sulfonamide group was incorporated in position 8 in order to explore possible H-bonding opportunities with the side chains of Lys58 and Asp102 in this region. Compound **7n** was obtained despite the synthetic difficulties, but no affinity improvement was gained. The crystal structure of **7n** indicated the presence of the predicted interactions: the sulfonamide group points toward the solvent and its nitrogen atom is hydrogen bonded to Asp102, while one of the two oxygen atom makes water mediated interactions with Lys58 and His154 (see Supporting information Fig. SI 5). On the other hand these interactions did not translate into an affinity improvement. The impact of the type and number of polar interactions introduced needs to be optimized experimentally, as the competing effects of binding and solvation are hardly predictable in quantitative terms.

Notwithstanding, molecular docking studies prompted us to design chemistry allowing the straightforward introduction of amines on C-8 to study the SAR of that position (Scheme 2). A number of analogues with different alkyl chains with polar ending, linked via an NH or a CO to position 8, were then synthesized and representative examples are shown in Table 3 (**12a–g** and **13a–b**). Ultimately, the hydroxyalkyl extension proved potent and soluble, compounds **12a** and **12b** being at least one order of magnitude more potent than the parent compound **7l**. We obtained an X-ray crystal structure of **12b** that confirmed the predicted binding mode and suggested that additional optimal

Table 3
Inhibitor activity against Hsp90 and cellular antiproliferative activity

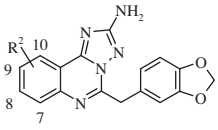

Compd	R^2	K_i (FP)[a] (μM)	A2780 IC_{50}[a] (μM)	LE[b]	Sol[c] (μM)
7l	H	0.035	10	0.43	6
7m	8-F	0.690	5.047	0.35	76
7n	8-SO_2NH_2	0.088	8.823	0.35	13
7o	10-F	0.005[d]	6.613	0.46	1
7p	8,10-diF	0.079	9.03	0.38	44
7q	10-Cl	>10			1
9a	8-OH	0.126	11	0.39	11
9b	7-OH	0.332	11.02	0.36	2
10b	8-NH_2	0.081	5.961	0.40	76
11	9-CH_2NH_2	>10	>10		117
12a	8-$NH(CH_2)_3OH$	0.001[d]	2.119	0.43	20
12b	8-$NH(CH_2)_2OH$	0.012	2.116	0.40	15
12c	8-$NH(CH_2)_2NH_2$	0.087	8.112	0.35	100
12d	8-$NH(CH_2)_2NMe_2$	0.03	9.189	0.35	205
12e	8-$NH(CH_2)_2$(pyrrolidine)	0.084	8.303	0.31	160
12f	8-MePiperazine	0.045	9.01	0.33	52
12g	8-$NH(CH_2)_2OMe$	0.064	3.60	0.36	14
13a	8-CONH-$(CH_2)_2$-OH	0.056	9.5	0.34	192
13b	8-CONH-$(CH_2)_3$-OH	0.034	8.19	0.34	51

[a] K_i (FP) values are an average of two or more determinations.
[b] Ligand efficiency LE = $-1.4\log(K_i)$/HAC; HAC = heavy atom count.
[c] Thermodynamic solubility pH 7 μM.
[d] Tight binding.

interactions were driving the enhanced inhibitory affinity, since all other interactions appeared conserved (Fig. 4A). In fact the 3-D structure of **12b** in complex with Hsp90 showed that position 8 is indeed the most solvent exposed of the scaffold. The hydrophilic OH group establishes a direct interactions with Asp102. This observation can be inferred to explain the improved potency of **12b** (K_i = 0.012 μM) over compound **12g** (K_i = 0.064 μM), which cannot make this contact. Similar considerations are also applicable for the C3 analog **12a**; molecular docking studies suggest an additional hydrophobic contact of the propyl chain with the Lys58 side chain that could explain the single digit nanomolar biochemical activity. Based on the crystal structure of **12b** it was hypothesized that incorporation of an amine into the alkyl chain, which would be protonated at physiological pH, could introduce an ionic interaction with Asp102, potentially providing increased affinity. To test these structure-based hypotheses, a series of aminoalkyl derivatives with a variety of hydrophilic moieties was prepared (Scheme 2). As reported in Table 3, the amino alkyl derivatives **12c–e** were less potent compared to the hydroxyl analogues. These observations are in contrast with the prediction, which did not take into account the energy balance of the solvation/desolvation step during the enzyme inhibitor binding process. Analogously, a larger substituent such as methyl piperazine in **12f** was found almost equipotent to **7l**.

Amide links of the aminopropanol and aminoethanol chains (**13a–b**) did not match the level of improvement observed with the corresponding amine junctions (**12a–b**), thus revealing the significant role played by the mode of substituent projection into the target space of this area, and the resultant inappropriate distance for the OH group to establish a direct interaction with Asp102.

Although the introduction of such a tether with polar endings improved the biochemical activity and solubility, an antiproliferative activity increase was observed only in a few cases (Table 3).

Compound **7o** described above showed the best ligand efficiency in this series, up to this point. Therefore, in order to enlarge the SAR around triazoloquinazoline derivatives, we combined the best performing 8-substitutions with the 10-fluoro core structure as reported in Table 4. Compound **17** was generally as effective as its parent counterparts (**7o** and **12f**) in inhibiting the Hsp90. Unfortunately, all the efforts to synthesize the desired compound with the best combination of 8-hydroxypropylamine with 10-F were vain.

We nonetheless envisioned further investigation of the 8–10 disubstitution pattern by working on synthon **7p** as reported in Scheme 3. The 8–10-difluoro aminotriazoloquinazoline **7p**, prepared from 3,5-difluoro anthranilic acid **4p**, proved to be a valuable intermediate in our strategies (Scheme 3). Thus, introduction of the solubilizing group was successfully achieved by thermal nucleophilic aromatic substitution on the 8,10-difluoro derivative **7p**, to deliver compounds **18a–e**. As previously mentioned (Scheme 3), ^{1}H NMR analysis indicated that they were the undesired regioisomers with the solubilizing group in position 10 and the fluorine atom in 8. However, upon testing, the compounds had residual Hsp90 inhibitory activity, although only **18a** performed decently (K_i = 0.179 μM).

Figure 4B shows a view of **18a** in the ligand binding pocket of Hsp90. Interestingly, the 3-D structure reveals once again an unexpected binding mode different from that of **12b**, where the aminotriazoloquinazoline moiety is flipped due to steric clashes induced by the *N*-alkyl substituent. The benzodioxole moiety points toward the solvent and makes a hydrogen bond with Lys58. The triazoloquinazoline ring fits into the induced hydrophobic pocket and, consequently, the aminotriazole NH_2 loses the key interaction with Asp93 and entails a hydrogen bond with the carbonyl group of Gly135, a specific feature in common with the bis-phenolic compound **8b** in the original binding mode of this class (Fig. 3A). The contribution of the fluorine atom seems to be essential for reaching activity (**18a** vs **14**) by occupying a small hydrophobic dimple defined by residues Val150 and Trp162 (electronic effects). The aminoethanol chain is located at the back of the induced pocket and extends into a narrow tunnel leading to the so called 'north opening' [25] with the hydroxyl group, displacing a conserved water molecule and mimicking its interaction with the side chain of Tyr139, Trp162 and the backbone carbonyl of Leu103. The structural information obtained for **18a** showed how this tunnel can be properly targeted by the ligand and offered another route for further compound optimization. A longer *N*-alkyl moiety or the methoxy capped tether abolished the activity (**18b** and **18c**), likely due to entropic effects or because these modifications would not include the interactions of the replaced water molecule.

Selected compounds with potent inhibitory activity in the Hsp90 biochemical assay were further characterized to establish that the antiproliferative activity measured so far was fully dependent on the inhibition of Hsp90. The Hsp90 dependent mechanism of action was monitored by following the depletion of the client protein Her2 (ErbB2) in BT474 cells supporting the premise that the antiproliferative activity was a consequence of chaperone inhibition (Table 5).

No activity was observed when the selected compounds were tested against the biologically related ATPase Hsc70 as well as against a panel of 56 protein kinases (IC_{50} >10 μM).[32]

Compound **12a** was further profiled and it demonstrated modest solubility (as measured in a high throughput thermodynamic solubility assay), moderate plasma protein binding and high

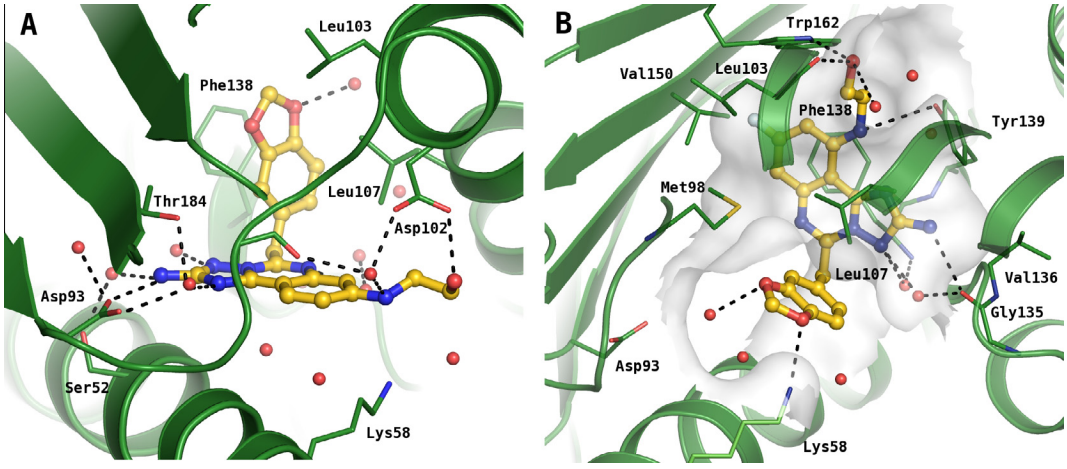

Figure 4. (A) Structure of **12b**. (B) The 'unexpected' binding mode of **18a** in HSP90.

Table 4
Biochemical and cellular values for analogues combining optimal substituents at the 8- and 10-positions

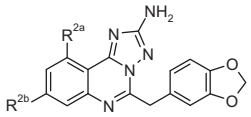

Compd	R^{2a}	R^{2b}	K_i (FP)[a] (μM)	A2780 IC_{50}[a] (μM)	LE	Sol[c] μM
12b	H	$NH(CH_2)_2OH$	0.012	2.116	0.40	15
14	$NH(CH_2)_2OH$	H	>5[d]			1
17	F	MePiperazine	0.009	1.55	0.33	38
18a	$NH(CH_2)_2OH$	F	0.179	6.516	0.33	23
18b	$NH(CH_2)_3OH$	F	>5	>10		2
18c	$NH(CH_2)_2OMe$	F	>5	>10		1
18d	$NH(CH_2)_2NH_2$	F	0.656	6.948	0.31	171
18e	MePiperazine	F	0.257	9.103	0.30	205

[a] K_i (FP) values are an average of two or more determinations.
[c] Thermodynamic solubility pH 7 μM.
[d] NMR K_i = 13.2 μM.

Table 5
Correlation between antiproliferative activity and mechanism of action

Compd	A2780 IC_{50}[a] (μM)	Her2 degrad IC_{50} (μM)
17	1.55	2.05
12a	2.119	2.56
12b	2.11	2.88
7o	6.313	6.706
10b	5.962	18.147
NVP-AUY922	0.001	0.010

[a] IC_{50} values are an average of two or more determinations.

Table 6
Physicochemical and ADME profile for compound **12a**[33]

PSA[a]	*c*Log*P*[b]	Sol[c]	Caco2_AB[d]	Caco2_ER[e]	PPB[f]	HLM[g]	RLM[g]	iv CL[h]	% Fos[i]
115.8	1.82	20	65.4	1	92.0	29.20	600	132	1.5

[a] Polar surface Area, calculated in A.[2]
[b] Calculated log*P*.
[c] Thermodynamic aqueous solubility, pH 7 (high throughput assay), in μg/mL.
[d] Apparent permeability apical (A) to basolateral (B) in 10^{-6} cm/s.
[e] Ratio of B < A/A < B permeability coefficients.
[f] Plasma protein binding human.
[g] Human or rat liver microsome intrinsic clearance, in mL/min/kg.
[h] Clearance in mice after 5 mg/kg iv injection, in mL/min/kg.
[i] Bioavailability in mice after 5 mg/kg oral dosing in 10% DMSO 0.1% Tween-20 in saline solution.[18]

permeability in a Caco2 assay. It was metabolically unstable both in vitro (human and rat liver microsomes) and in vivo, with poor oral bioavailability in mice. The reason for low bioavailability may be attributed to the high first pass metabolism supported by the high microsome turnover measured (see Table 6).

4. Conclusion

In summary, the application of a fragment-based approach with FAXS NMR support allowed us to identify aminotriazoloquinazolines as a new Hsp90 inhibitor chemotype. Starting from aminotriazoloquinazoline fragment **3** (FAXS NMR K_i = 32.2 μM, LE = 0.37), X-ray crystallographic data were used to establish key determinants for affinity and to guide structure-based design. In particular, a strategy of fragment growing based on structural data, computational analysis and medicinal chemistry led to **12a** as a promising lead with a 30,000-fold gain in activity, relative to starting point **3**, possessing a good LE, which was maintained during optimization. Moreover, the identification of derivatives with new unexpected binding modes opened opportunities to develop different chemical optimization pathways and eventually different chemical series based on the same chemical scaffold. Further optimization of **12a** is ongoing in order to improve its ADME properties.

5. Experimental

5.1. Chemistry

All solvents and reagents, unless otherwise stated, were commercially available, of the best grade and were used without further purification. All experiments dealing with moisture-sensitive compounds were carried out under dry nitrogen or argon atmosphere. Thin-layer chromatography was performed on Merck Silica Gel 60 F254 pre-coated plates. Column chromatography was conducted under medium pressure on silica (Merck Silica Gel 40–63 μm). ^{1}H NMR spectra were recorded on a Varian INOVA 400 spectrometer (operating at 400.5 MHz for ^{1}H) and equipped with a 5 mm ^{1}H{^{13}C–^{15}N} *z* axis PFG indirect detection probe. Chemical shifts were referenced with respect to the residual solvents signals.[34] Data are reported as follows: chemical shift (δ, ppm), multiplicity (s = singlet, d = doublet, t = triplet, q = quartet, br s = broad signal, td = triplet of doublet, dd = doublet of doublets, ddd = doublet of doublets of doublets, m = multiplet), coupling constants (Hz), and number of protons. Electrospray (ESI) mass spectra were obtained on a Finnigan LCQ ion trap. HPLC–UV–MS analyses were carried out combining the ion trap MS instrument with HPLC system SSP4000 (Thermo Separation Products) equipped with an auto-sampler LC Pal (CTC Analytics) and UV6000LP diode array detector (UV detection 215–400 nm). Instrument control, data acquisition and processing were performed by using Xcalibur 1.2 software (Finnigan). HPLC chromatography was run at room temperature, and 1 mL/min flow rate, using a Waters X Terra RP 18 column (4.6 × 50 mm; 3.5 μm). Mobile phase A was ammonium acetate 5 mM buffer (pH 5.5 with acetic acid)/acetonitrile 90:10, and mobile phase B was ammonium acetate 5 mM buffer (pH 5.5 with acetic acid)/acetonitrile 10:90; the gradient was from 0% to 100% B in 7 min then hold 100% B for 2 min before re-equilibration. Mass data given as *m*/*z* ratio. ESI(+) high resolution mass spectra (HRMS) were obtained on a Waters Q-Tof Ultima directly connected with a micro HPLC 1100 Agilent as previously described.[35]

5.1.1. General procedure for preparation of compounds 7a–7d

A solution of 2-aminobenzoic acid derivatives **4** (1.2 mmol), and butyric anhydride (1 mL) was heated under microwave condition at 160 °C for 5 min. The mixture was diluted with dichloromethane and washed with $NaHCO_3$ saturated solution, then with water followed by brine. The organic phase was dried over Na_2SO_4, filtered and evaporated to give the benzo[*d*][1,3]oxazin-4-one intermediates **6a**–**d**. To a solution of benzo[*d*][1,3]oxazin-4-ones **6** (0.62 mmol) in dry pyridine (2 mL) was added aminoguanidine hydrogencarbonate (1.2 mmol) and the mixture was heated under microwave condition at 180 °C for 20 min (Warning high pressure was developed). The solvent was then evaporated and the crude was diluted with MeOH or a mixture of MeOH/H_2O 1:1. The compounds precipitated, after filtration they were washed with MeOH to afford the title compounds as solid.

5.1.2. 7-Methoxy-5-propyl[1,2,4]triazolo[1,5-*c*]quinazolin-2-amine 7a

Yield 30% as an off-white solid. ^{1}H NMR (400 MHz, DMSO-d_6) δ 7.73 (dd, J = 8.0, 1.2 Hz, 1H), 7.57 (t, J = 8.0 Hz, 1H), 7.32 (dd, J = 8.0, 1.2 Hz, 1H), 6.41 (s, 2H), 3.96 (s, 3H), 3.11 (t, J = 7.5 Hz, 2H), 1.89 (sxt, J = 7.5 Hz, 2H), 1.01 (t, J = 7.5 Hz, 3H). LCMS: m/z 258 $[M+H]^+$ at rt 3.66 min; HRMS (ESI) calcd for $C_{13}H_{16}N_5O$ $[M+H]^+$ 258.135 found 258.1358.

5.1.3. 10-Fluoro-5-propyl[1,2,4]triazolo[1,5-*c*]quinazolin-2-amine 7b

Yield 14% as an off-white solid. ^{1}H NMR (400 MHz, DMSO-d_6) δ 7.78 (ddd, J = 8.3, 7.9, 5.7 Hz, 1H), 7.72 (dd, J = 8.3, 1.1 Hz, 1H), 7.47 (ddd, J = 10.2, 7.9, 1.1 Hz, 1H), 6.54 (br s, 2H), 3.13 (dd, J = 7.7, 7.4 Hz, 2H), 1.91 (sxt, J = 7.5 Hz, 2H), 1.02 (t, J = 7.5 Hz, 3H). LCMS: m/z 246 $[M+H]^+$ at rt 4.02 min; HRMS (ESI) calcd for $C_{12}H_{13}FN_5$ $[M+H]^+$ 246.115 found 246.1152.

5.1.4. 7-Methyl-5-propyl[1,2,4]triazolo[1,5-*c*]quinazolin-2-amine 7c

Yield 7% as an off-white solid. ^{1}H NMR (400 MHz, DMSO-d_6) δ 8.04 (dd, J = 8.0, 1.4 Hz, 1H), 7.67 (dd, J = 7.3, 1.4 Hz, 1H), 7.53 (dd, J = 8.0, 7.3 Hz, 1H), 6.40 (br s, 2H), 3.13 (t, J = 7.5 Hz, 2H), 2.67 (s, 3H), 1.94 (sxt, J = 7.4 Hz, 2H), 1.05 (t, J = 7.4 Hz, 3H). LCMS: m/z 242 $[M+H]^+$ at rt 5.36 min; HRMS (ESI) calcd for $C_{13}H_{16}N_5$ $[M+H]^+$ 242.14 found 242.1409.

5.1.5. 7-Chloro-5-propyl[1,2,4]triazolo[1,5-*c*]quinazolin-2-amine 7d

Yield 11% as an off-white solid. ^{1}H NMR (400 MHz, DMSO-d_6) δ 8.17 (dd, J = 8.0, 1.3 Hz, 1H), 7.96 (dd, J = 7.8, 1.3 Hz, 1H), 7.62 (dd, J = 8.0, 7.8 Hz, 1H), 6.53 (br s, 2H), 3.15 (t, J = 7.7 Hz, 2H), 1.94 (sxt, J = 7.5 Hz, 2H), 1.05 (t, J = 7.5 Hz, 3H). LCMS: m/z 262 $[M+H]^+$ at rt 5.05 min; HRMS (ESI) calcd for $C_{12}H_{13}ClN_5$ $[M+H]^+$ 262.0854 found 262.0851.

5.1.6. General procedure for preparation of compounds 7e–7p

To a solution of acyl chlorides (18.70 mmol) in anhydrous dichloromethane (20 mL) was added 2-amino-benzoic acid derivatives **4** (12.5 mmol). After the addition of pyridine (5 mL), the mixture was heated under microwave condition at 120 °C for 5 min. The solvent was evaporated and the residue was diluted with 2 N HCl solution to induce the precipitation of a brown solid which was filtered, washed with water and dried under vacuum at 50 °C, to afford the 2-acylamine-benzoic acids **5**. A stirred solution of compounds **5** (25 mmol) in acetic anhydride (50 mL) was refluxed for 10 min. The solvent was removed in vacuum and the residue was taken up in diethyl ether, to provide after filtration and drying the title benzoxazin-4-ones **6**. A solution of benzoxazin-4-ones **6** (20.2 mmol) and aminoguanidine hydrogencarbonate (20.2 mmol) in pyridine (25 mL) was heated under microwave condition at 180 °C for 30 min. The reaction was cooled at room temperature and diluted with methanol/water 1:1 to induce the precipitation of a brown solid which was washed with a mixture MeOH/H_2O 8:2, to afford the desired compounds.

5.1.7. 5-[2-(4-Methoxyphenyl)ethyl][1,2,4]triazolo[1,5-*c*]quinazolin-2-amine 7e

Yield 22% as an off-white solid. ^{1}H NMR (400 MHz, DMSO-d_6) δ 8.21 (dd, J = 8.0, 0.8 Hz, 1H), 7.91 (d, J = 8.3 Hz, 1H), 7.81 (ddd, J = 8.0, 7.2, 1.5 Hz, 1H), 7.66 (ddd, J = 8.3, 7.2, 1.0 Hz, 1H), 7.22 (d, J = 8.7 Hz, 2H), 6.85 (d, J = 8.7 Hz, 2H), 6.44 (br s, 2H), 3.71 (s, 3H), 3.41 (t, J = 8.0 Hz, 2H), 3.17 (t, J = 8.0 Hz, 2H). LCMS: m/z 320 $[M+H]^+$ at rt 5.90 min; HRMS (ESI) calcd for $C_{18}H_{18}N_5O$ $[M+H]^+$ 320.1506 found 320.1512.

5.1.8. 5-[2-(3-Nitrophenyl)ethyl][1,2,4]triazolo[1,5-*c*]quinazolin-2-amine 7f

Yield 30% as an orange solid. ^{1}H NMR (400 MHz, DMSO-d_6) δ 8.23 (t, J = 1.8 Hz, 1H), 8.21 (ddd, J = 7.9, 1.5, 0.5 Hz, 1H), 8.06 (ddd, J = 8.2, 2.3, 1.0 Hz, 1H), 7.79–7.84 (m, 2H), 7.90 (ddd, J = 8.4, 1.2, 0.5 Hz, 1H), 7.67 (ddd, J = 8.0, 7.1, 1.2 Hz, 1H), 7.59 (t, J = 7.9 Hz, 1H), 6.45 (br s, 2H), 3.53 (m, 2H), 3.41 (t, J = 7.7 Hz, 2H).

5.1.9. 5-(4-Methoxybenzyl)[1,2,4]triazolo[1,5-*c*]quinazolin-2-amine 7g

Yield 38% as an off-white solid. ^{1}H NMR (400 MHz, DMSO-d_6) δ 8.21 (dd, J = 7.9, 1.0 Hz, 1H), 7.90 (d, J = 7.6 1.0 Hz, 1H), 7.81 (td, J = 7.6, 1.5 Hz, 1H), 7.67 (td, J = 7.9, 7.6, 1.0 Hz, 1H), 7.33 (d, J = 8.8 Hz, 2H), 6.88 (d, J = 8.8 Hz, 2H), 6.46 (s, 2H), 4.45 (s, 2H), 3.72 (s, 3H). LCMS: m/z 306 $[M+H]^+$ at rt 4.51 min; HRMS (ESI) calcd for $C_{17}H_{16}N_5O$ $[M+H]^+$ 306.135 found 306.1352.

5.1.10. 5-(3,5-Dimethoxybenzyl)[1,2,4]triazolo[1,5-*c*]quinazolin-2-amine 7h

Yield 14% as an off-white solid. ^{1}H NMR (400 MHz, DMSO-d_6) δ 8.21 (ddd, J = 8.1, 1.3, 0.6 Hz, 1H), 7.90 (m, 1H), 7.81 (ddd, J = 8.4, 7.1, 1.5 Hz, 1H), 7.67 (ddd, J = 8.1, 7.1, 1.0 Hz, 1H), 6.55 (d, J = 2.2 Hz, 2H), 6.47 (br s, 2H), 6.38 (t, J = 2.3 Hz, 1H), 4.44 (s, 2H), 3.69 (s, 6H). LCMS: m/z 336 $[M+H]^+$ at rt 4.62 min; HRMS (ESI) calcd for $C_{18}H_{18}N_5O_2$ $[M+H]^+$ 336.1455 found 336.1457.

5.1.11. 5-(2,4-Dimethoxybenzyl)[1,2,4]triazolo[1,5-*c*]quinazolin-2-amine 7i

Yield 13% as a light yellow solid. ^{1}H NMR (400 MHz, DMSO-d_6) δ 8.22 (ddd, J = 8.0, 1.4, 0.6 Hz, 1H), 7.80 (m, 1H), 7.77 (m, 1H), 7.66 (ddd, J = 8.0, 6.4, 2.0 Hz, 1H), 6.98 (d, J = 8.3 Hz, 1H), 6.59 (d, J = 2.4 Hz, 1H), 6.44 (dd, J = 8.3, 2.4 Hz, 1H), 6.43 (br s, 2H), 4.39 (s, 2H), 3.75 (s, 3H), 3.72 (s, 3H). LCMS: m/z 336 $[M+H]^+$ at rt 4.74 min; HRMS (ESI) calcd for $C_{18}H_{18}N_5O_2$ $[M+H]^+$ 336.1455 found 336.1454.

5.1.12. 5-(2,5-Dimethoxybenzyl)[1,2,4]triazolo[1,5-*c*]quinazolin-2-amine 7j

Yield 30% as an off-white solid. ^{1}H NMR (400 MHz, DMSO-d_6) δ 8.22 (ddd, J = 7.8, 1.2, 0.7 Hz, 1H), 7.80 (m, 1H), 7.77 (m, 1H), 7.66 (ddd, J = 8.3, 7.8, 1.6 Hz, 1H), 6.95 (d, J = 8.9 Hz, 1H), 6.82 (dd, J = 8.9, 2.9 Hz, 1H), 6.73 (d, J = 2.9 Hz, 1H), 6.45 (br s, 2H), 4.45 (s, 1H), 3.67 (s, 3H), 3.65 (s, 3H). LCMS: m/z 336 $[M+H]^+$ at rt 4.70 min; HRMS (ESI) calcd for $C_{18}H_{18}N_5O_2$ $[M+H]^+$ 336.1455 found 336.1452.

5.1.13. 5-(3,4-Dimethoxybenzyl)[1,2,4]triazolo[1,5-*c*]quinazolin-2-amine 7k

Yield 23% as an off-white solid. ^{1}H NMR (400 MHz, DMSO-d_6) δ 8.21 (ddd, J = 7.9, 1.5, 0.6 Hz, 1H), 7.89 (ddd, J = 8.3, 1.4, 0.6 Hz, 1H),

7.80 (ddd, J = 8.3, 7.9, 1.4 Hz, 1H), 7.66 (ddd, J = 8.3, 8.2, 1.2 Hz, 1H), 7.09 (s, 1H), 6.86 (s, 2H), 6.46 (s, 2H), 4.44 (s, 2H), 3.72 (s, 3H), 3.70 (s, 3H). LCMS: m/z 336 $[M+H]^+$ at rt 5.08 min; HRMS (ESI) calcd for $C_{18}H_{18}N_5O_2$ $[M+H]^+$ 336.1455 found 336.1443.

5.1.14. 5-(1,3-Benzodioxol-5-ylmethyl)[1,2,4]triazolo[1,5-*c*]quinazolin-2-amine 7l

Yield 23% as an off-white solid. ^{1}H NMR (400 MHz, DMSO-d_6) δ 8.21 (ddd, J = 8.1, 1.3, 0.5 Hz, 1H), 7.88 (ddd, J = 8.3, 1.0, 0.5 Hz, 1H), 7.80 (ddd, J = 8.4, 7.1, 1.5 Hz, 1H), 7.67 (ddd, J = 8.0, 7.1, 1.2 Hz, 1H), 7.00 (d, J = 1.0 Hz, 1H), 6.85 (m, 1H), 6.83 (m, 1H), 6.47 (br s, 2H), 5.96 (s, 2H), 4.42 (s, 2H). LCMS: m/z 320 $[M+H]^+$ at rt 4.62 min; HRMS (ESI) calcd for $C_{17}H_{14}N_5O_2$ $[M+H]^+$ 320.1142 found 320.1136.

5.1.15. 5-(1,3-Benzodioxol-5-ylmethyl)-8-fluoro[1,2,4]triazolo[1,5-*c*]quinazolin-2-amine 7m

Yield 9% as an off-white solid. ^{1}H NMR (400 MHz, DMSO-d_6) δ 8.26 (dd, J = 8.9, 6.1 Hz, 1H), 7.68 (dd, J = 10.3, 2.5 Hz, 1H), 7.56 (td, J = 8.8, 2.6 Hz, 1H), 6.99 (br s, 1H), 6.84 (m, 2H), 6.51 (s, 2H), 5.97 (s, 2H), 4.42 (s, 2H). LCMS: m/z 338 $[M+H]^+$ at rt 5.51 min; HRMS (ESI) calcd for $C_{17}H_{13}FN_5O_2$ $[M+H]^+$ 338.1048 found 338.1051.

5.1.16. 5-(1,3-Benzodioxol-5-ylmethyl)-10-fluoro[1,2,4]triazolo[1,5-*c*]quinazolin-2-amine 7o

Yield 14% as a grey solid. ^{1}H NMR (400 MHz, DMSO-d_6) δ 7.78 (ddd, J = 11.3, 8.3, 5.7 Hz, 1H), 7.72 (m, 1H), 7.49 (m, 1H), 7.00 (s, 1H), 6.81–6.88 (m, 2H), 6.59 (s, 2H), 5.98 (s, 2H), 4.44 (s, 2H). LCMS: m/z 338 $[M+H]^+$ at rt 5.45 min; HRMS (ESI) calcd for $C_{17}H_{13}FN_5O_2$ $[M+H]^+$ 338.1048 found 338.1038.

5.1.17. 5-(1,3-Benzodioxol-5-ylmethyl)-8,10-difluoro[1,2,4]triazolo[1,5-*c*]quinazolin-2-amine 7p

Yield 14% as an off-white solid. ^{1}H NMR (400 MHz, DMSO-d_6) δ 7.53–7.65 (m, 2H), 6.98 (s, 1H), 6.84 (m, 2H), 6.63 (s, 2H), 5.97 (s, 2H), 4.42 (s, 2H). LCMS: m/z 356 $[M+H]^+$ at rt 5.8 min; HRMS (ESI) calcd for $C_{17}H_{12}F_2N_5O_2$ $[M+H]^+$ 356.0954 found 356.0966.

5.1.18. 5-(1,3-Benzodioxol-5-ylmethyl)-10-chloro[1,2,4]triazolo[1,5-*c*]quinazolin-2-amine 7q

Yield 8% as an off-white solid. ^{1}H NMR (400 MHz, DMSO-d_6) δ 7.85 (m, 1H), 7.75 (m, 2H), 7.00 (s, 1H), 6.85 (m, 2H), 6.58 (s, 2H), 5.98 (s, 2H), 4.45 (s, 2H). LCMS: m/z 354 $[M+H]^+$ at rt 5.99 min; HRMS (ESI) calcd for $C_{17}H_{13}ClN_5O_2$ $[M+H]^+$ 354.0753 found 354.0753.

5.1.19. 5-(1,3-Benzodioxol-5-ylmethyl)-8-[(4-methoxybenzyl)oxy][1,2,4]triazolo[1,5-*c*]quinazolin-2-amine 7r

Yield 13% as brown solid. LCMS: m/z 456 $[M+H]^+$ at rt 6.01 min.

5.1.20. 5-(1,3-Benzodioxol-5-ylmethyl)-7-[(4-methoxybenzyl)oxy][1,2,4]triazolo[1,5-*c*]quinazolin-2-amine 7s

Yield 10% as brown solid. LCMS: m/z 456 $[M+H]^+$ at rt 6.10 min.

5.1.21. 2-Amino-5-(1,3-benzodioxol-5-ylmethyl)[1,2,4]triazolo[1,5-*c*]quinazoline-9-carbonitrile 7t

Yield 26% as brown solid. ^{1}H NMR (400 MHz, DMSO-d_6) δ 8.65 (dd, J = 1.9, 0.5 Hz, 1H), 8.12 (dd, J = 8.7, 2.0 Hz, 1H), 8.01 (dd, J = 8.7, 0.5 Hz, 1H), 7.00 (d, J = 0.9 Hz, 1H), 6.85 (m, 2H), 6.67 (s, 2H), 5.97 (s, 2H), 4.46 (s, 2H).

5.1.22. 5-Benzo[1,3]dioxol-5-ylmethyl-[1,2,4]triazolo[1,5-*c*]quinazoline-8-nitro-2-ylamine 7u

Yield 27% as yellow solid. ^{1}H NMR (400 MHz, DMSO-d_6) δ 8.61 (dd, J = 2.1, 0.6 Hz, 1H), 8.43 (dd, J = 8.9, 0.6 Hz, 1H), 8.41 (dd, J = 8.9, 2.1 Hz, 1H), 7.02 (d, J = 1.1 Hz, 1H), 6.88 (m, 1H), 6.85 (m, 1H), 6.71 (s, 2H), 5.98 (s, 2H), 4.48 (s, 2H).

5.1.23. 2-Amino-5-(1,3-benzodioxol-5-ylmethyl)[1,2,4]triazolo[1,5-*c*]quinazoline-8-carboxylic acid 7v

Yield 41% as grey solid. LCMS: m/z 364 $[M+H]^+$ at rt 4.06 min.

5.1.24. 2-Amino-5-benzo[1,3]dioxol-5-ylmethyl-[1,2,4]triazolo[1,5-*c*]quinazoline-8-sulfonic acid amide 7n

To a solution of benzo[1,3]dioxol-5-yl-acetic acid (0.18 g, 1 mmol) in dry *N*,*N*-dimethylformamide (15 mL), 1,1-carbonyldiimidazole (0.18 g, 1.1 mmol) was added. The mixture was stirred at room temperature for 1 h, then 2-amino-4-sulfamoyl-benzoic acid (0.22 g, 1 mmol) was added portion wise. The reaction was stirred at room temperature for 2 days, diluted with dichloromethane and washed with 1 N HCl solution, then with water and brine. The organic phase was dried over Na_2SO_4, filtered and evaporated to give a crude that was purified by flash column chromatography on silica gel eluting with ethyl acetate/hexane 8:2, to afford 2-(2-benzo[1,3]dioxol-5-yl-acetylamino)-4-sulfamoyl-benzoic acid (0.20 g, 53% yield). ^{1}H NMR (400 MHz, DMSO-d_6) δ 14.62 (br s, 1H), 12.24 (br s, 1H), 8.93 (d, 1H), 8.09 (d, 1H), 7.37 (dd, 1H), 7.25 (br s, 2H), 6.90 (d, 1H), 6.85 (d, 1H), 6.80 (dd, 1H), 5.97 (s, 2H), 3.54 (br s, 2H). A mixture of the compound (0.10 g, 0.26 mmol), acetic acid (1.5 mL) and acetic anhydride (0.10 mL, 1.06 mmol) was stirred at reflux for 1 h. The reaction was diluted with ethyl acetate and washed with $NaHCO_3$ saturated solution, then with water and brine. The organic phase was dried over Na_2SO_4, filtered and evaporated to give the 2-benzo[1,3]dioxol-5-ylmethyl-4-oxo-4*H*-benzo[*d*][1,3]oxazine-7-sulfonic acid amide intermediate (0.032 g) as yellow oil. To a solution of 2-benzo[1,3]dioxol-5-ylmethyl-4-oxo-4*H*-benzo[*d*][1,3]oxazine-7-sulfonic acid amide (0.032 g, 0.09 mmol) in dry pyridine (1 mL) was added aminoguanidine hydrogencarbonate (0.013 g, 0.098 mmol) and the mixture was heated under microwave condition at 180 °C for 1.5 h. The solvent was then evaporated and the crude was taken up in methanol to give the title compound (0.013 g, 37% yield). ^{1}H NMR (400 MHz, DMSO-d_6) δ 8.38 (d, J = 8.4 Hz, 1H), 8.25 (d, J = 1.5 Hz, 1H), 8.01 (dd, J = 8.4, 1.5 Hz, 1H), 7.59 (s, 2H), 7.01 (d, 1H), 6.85 (m, 2H), 6.60 (s, 2H), 5.98 (s, 2H), 4.46 (s, 2H). LCMS: m/z 399 $[M+H]^+$ at rt 4.68 min; HRMS (ESI) calcd for $C_{17}H_{15}N_6O_4S$ $[M+H]^+$ 399.087 found 399.0884.

5.1.25. 4-[2-(2-Amino[1,2,4]triazolo[1,5-*c*]quinazolin-5-yl)ethyl]phenol 8a

To a stirred solution of **7e** (145 mg, 0.48 mmol) in DCM (5 mL) was slowly added 1 M BBr_3 in DCM (4.86 mL, 4.86 mmol) at 0 °C and left on stirring for 2 h at room temperature, the cloudy solution was then diluted with water and partitioned with EtOAc, washed with $NaHCO_3$ saturated solution, then with water and brine. The organic phase was dried over Na_2SO_4. The solvent was removed and the residue was washed with diethylether to afford **8a** as a white solid (90 mg, 48%). ^{1}H NMR (400 MHz, DMSO-d_6) δ 9.16 (s, 1H), 8.22 (dd, J = 8.0, 0.9 Hz, 1H), 7.92 (d, J = 7.2 Hz, 1H), 7.82 (td, J = 7.7, 1.5 Hz, 1H), 7.67 (dd, J = 8.0, 1.9 Hz, 1H), 7.09 (d, J = 8.5 Hz, 2H), 6.68 (d, J = 8.5 Hz, 2H), 6.45 (s, 2H), 3.40 (m, 2H), 3.12 (m, 2H). LCMS: m/z 306 $[M+H]^+$ at rt 3.93 min; HRMS (ESI) calcd for $C_{17}H_{16}N_5O$ $[M+H]^+$ 306.135 found 306.1353.

5.1.26. 5-(2-Amino-[1,2,4]triazolo[1,5-*c*]quinazolin-5-ylmethyl)-benzene-1,3-diol 8b

To a stirred suspension of **7g** (0.10 g, 0.30 mmol), in anhydrous dichloromethane (10 mL) was added dropwise, under argon, 1 M BBr_3 solution (3 mL, 3 mmol) in DCM at 0–5 °C. The ice bath was removed and the mixture was stirred at room temperature overnight. The reaction was diluted with ethyl acetate and washed with $NaHCO_3$ saturated solution, then with water and brine. After

drying over Na_2SO_4, the solvent was removed to give a crude that was crystallized twice from ethyl acetate to afford the title compound as a white solid (0.70 g, 70% yield). ^{1}H NMR (400 MHz, DMSO-d_6) δ 9.12 (s, 2H), 8.22 (d, J = 7.9 Hz, 1H), 7.91 (d, J = 8.3 Hz, 1H), 7.82 (td, J = 7.7, 1.3 Hz, 1H), 7.68 (t, J = 7.5 Hz, 1H), 6.45 (br s, 2H), 6.18 (d, J = 2.1 Hz, 2H), 6.05 (t, J = 2.1 Hz, 1H), 4.32 (s, 2H). LCMS: m/z 308 $[M+H]^+$ at rt 4.05 min; HRMS (ESI) calcd for $C_{16}H_{14}N_5O_2$ $[M+H]^+$ 308.1142 found 308.1137. The following compound **8c** was prepared according to the method described above.

5.1.27. 4-(2-Amino-[1,2,4]triazolo[1,5-*c*]quinazolin-5-ylmethyl)-benzene-1,3-diol 8c

Yield 76% as a white solid. ^{1}H NMR (400 MHz, DMSO-d_6) δ 9.33 (s, 1H), 9.10 (s, 1H), 8.21 (ddd, J = 7.9, 1.3, 0.6 Hz, 1H), 7.81 (ddd, J = 8.4, 1.5, 0.5 Hz, 1H), 7.77 (ddd, J = 8.3, 6.8, 1.5 Hz, 1H), 7.65 (ddd, J = 8.0, 6.7, 1.6 Hz, 1H), 6.80 (d, J = 8.2 Hz, 1H), 6.45 (br s, 2H), 6.32 (m, 1H), 6.14 (dd, J = 8.2, 2.4 Hz, 1H), 4.32 (s, 2H). LCMS: m/z 308 $[M+H]^+$ at rt 3.41 min; HRMS (ESI) calcd for $C_{16}H_{14}N_5O_2$ $[M+H]^+$ 308.1142 found 308.1136.

5.1.28. 2-Amino-5-benzo[1,3]dioxol-5-ylmethyl-[1,2,4]triazolo[1,5-*c*]quinazolin-8-ol 9a

To a stirred solution of **7s** (20 mg, 0.043 mmol) in 1,4-dioxane (1 mL) was added 4 N HCl in dioxane (1 mL). The reaction mixture was stirred for 1 h, the solvent removed, the residue was triturated with diethyl ether, the crude was submitted to preparative HPLC to afford the title product (7 mg, 50%). ^{1}H NMR (400 MHz, DMSO-d_6) δ 10.39 (br s, 1H), 8.03 (d, J = 8.5 Hz, 1H), 7.08–7.18 (m, 2H), 6.98 (s, 1H), 6.83 (m, 2H), 6.35 (br s, 2H), 5.96 (s, 2H), 4.36 (s, 2H). LCMS: m/z 336 $[M+H]^+$ at rt 3.57 min; HRMS (ESI) calcd for $C_{17}H_{14}N_5O_3$ [M+H336.1091 found 336.1085. The following compound **9b** was prepared according to the method described above.

5.1.29. 2-Amino-5-benzo[1,3]dioxol-5-ylmethyl-[1,2,4]triazolo[1,5-*c*]quinazolin-7-ol 9b

Yield 17% as a white solid. ^{1}H NMR (400 MHz, DMSO-d_6) δ 9.87 (s, 1H), 7.60 (dd, J = 7.9, 1.3 Hz, 1H), 7.47 (t, J = 7.9 Hz, 1H), 7.19 (dd, J = 7.9, 1.3 Hz, 1H), 7.07 (d, J = 1.3 Hz, 1H), 6.87 (dd, J = 7.9, 1.6 Hz, 1H), 6.82 (d, J = 7.9 Hz, 1H), 6.43 (br s, 2H), 5.95 (s, 2H), 4.41 (s, 2H). LCMS: m/z 336 $[M+H]^+$ at rt 5.27 min; HRMS (ESI) calcd for $C_{17}H_{14}N_5O_3$ [M+H336.1091 found 336.1094.

5.1.30. 5-[2-(3-Aminophenyl)ethyl][1,2,4]triazolo[1,5-*c*]quinazolin-2-amine 10a

To a solution of **7f** (0.10 g, 0.29 mmol) was dissolved in *N*,*N*-dimethylformamide (10 mL), and 10% Pd/C (50% w/w, 0.05 g) was added. The mixture was reacted in Parr Apparatus at 40 p.s.i. for 5 h. The suspension was filtered through Celite®. After washing the filter with methanol, the solution was evaporated to dryness. The crude was twice crystallized from ethyl acetate to provide the title product as a tan solid (0.062 g, 67% yield). ^{1}H NMR (DMSO-d_6,400 MHz): δ 8.21 (ddd, J = 8.1, 1.3, 0.6 Hz, 1H), 7.91 (m, 1H), 7.81 (ddd, J = 8.4, 7.0, 1.5 Hz, 1H), 7.66 (ddd, J = 8.0, 7.1, 1.2 Hz, 1H), 6.92 (t, J = 7.7 Hz, 1H), 6.51 (t, J = 1.8 Hz, 1H), 6.44 (br s, 2H), 6.44 (m, 1H), 6.39 (ddd, J = 8.0, 2.2, 0.9 Hz, 1H), 4.95 (br s, 2H), 3.39 (m, 2H), 3.06 (m, 2H). LCMS: m/z 305 $[M+H]^+$ at rt 4.06 min; HRMS (ESI) calcd for $C_{17}H_{17}N_6$ $[M+H]^+$ 305.1509 found 305.1502.

5.1.31. 5-(1,3-Benzodioxol-5-ylmethyl)[1,2,4]triazolo[1,5-*c*]quinazoline-2,8-diamine 10b

To a solution of **7u** (0.05 g, 0.137 mmol), in *N*,*N*-dimethylformamide (4 mL), 10% Pd/C (10% w/w, 0.03 g) and cyclohexane (1 mL) were added. The mixture was heated under microwave condition at 100 °C for 2 h. The suspension was filtered through Celite®. After washing the filter with methanol, the solution was evaporated to dryness. The crude was twice crystallized from diethyl ether to provide the title product as a light brown solid (0.020 g, 44% yield). ^{1}H NMR (400 MHz, DMSO-d_6) δ 7.84 (d, J = 8.7 Hz, 1H), 6.98 (m, 1H), 6.93 (dd, J = 8.7, 2.1 Hz, 1H), 6.85 (d, J = 2.0 Hz, 1H), 6.83 (m, 2H), 6.21 (s, 2H), 5.97 (s, 2H), 5.94 (br s, 2H), 4.31 (s, 2H). LCMS: m/z 335 $[M+H]^+$ at rt 4.55 min; HRMS (ESI) calcd for $C_{17}H_{15}N_6O_2$ $[M+H]^+$ 335.1251 found 335.1262.

5.1.32. 9-(Aminomethyl)-5-(1,3-benzodioxol-5-ylmethyl)[1,2,4]triazolo[1,5-*c*]quinazolin-2-amine 11

The compound **7t** (0.07 g, 0.20 mmol) was dissolved in a mixture of tetrahydrofuran (5 mL) and methanol (5 mL) followed by sequential addition of cobalt(II) chloride (0.11 g, 0.81 mmol) and sodium borohydride (0.03 g, 0.81 mmol). The reaction was stirred at room temperature overnight, then the solvent was evaporated. The residue was dissolved in $CHCl_3$/CH_3OH 9:1 and washed with ammonium hydroxide solution (pH 12). The organic phase was dried over Na_2SO_4, filtered and evaporated to obtain a crude, which was purified by preparative HPLC to give the title compound (0.01 g, 7% yield). ^{1}H NMR (400 MHz, DMSO-d_6) δ 8.16 (d, J = 1.2 Hz, 1H), 7.81 (d, J = 8.3 Hz, 1H), 7.75 (dd, J = 8.5, 2.0 Hz, 1H), 6.99 (s, 1H), 6.81–6.87 (m, 2H), 6.42 (s, 2H), 5.96 (s, 2H), 4.41 (s, 2H), 3.92 (s, 2H). LCMS: m/z 349 $[M+H]^+$ at rt 3.06 min; HRMS (ESI) calcd for $C_{18}H_{17}N_6O_2$ $[M+H]^+$ 349.1408 found 349.1425.

5.1.33. General procedure for preparation of compounds 12a–g

To 5-benzo[1,3]dioxol-5-ylmethyl-8-fluoro-[1,2,4]triazolo[1,5-*c*] quinazolin-2-ylamine **7m** (0.05 g, 0.15 mmol), amine derivative (0.7 mL) was added and the mixture was heated at 140 °C for 2–8 h. The reaction was cooled at room temperature and the precipitated solid was filtered and washed with a mixture MeOH/H_2O 9:1, to provide the desired compounds.

5.1.34. 2-Amino-5-benzo[1,3]dioxol-5-ylmethyl-[1,2,4]triazolo[1,5-*c*]quinazolin-8-ylamino)-propan-1-ol 12a

Yield 66% as an off-white solid. ^{1}H NMR (400 MHz, DMSO-d_6) δ 7.84 (d, J = 8.8 Hz, 1H), 6.98(dd, J = 8.8, 2.6 Hz, 1H), 6.97 (d, J = 1.0 Hz, 1H), 6.83 (d, J = 1.0 Hz, 2H), 6.72 (d, J = 2.2 Hz, 1H), 6.49 (t, J = 5.4 Hz, 1H), 6.21 (s, 2H), 5.96 (s, 2H), 4.50 (t, J = 5.1 Hz, 1H), 4.31 (s, 2H), 3.53 (q, J = 6.1 Hz, 2H), 3.18 (q, J = 6.5 Hz, 2H), 1.74 (quin, J = 6.6 Hz, 2H). LCMS: m/z 393 $[M+H]^+$ at rt 4.64 min; HRMS (ESI) calcd for $C_{20}H_{21}N_6O_3$ $[M+H]^+$ 393.167 found 393.1684.

5.1.35. 2-(2-Amino-5-benzo[1,3]dioxol-5-ylmethyl-[1,2,4]triazolo[1,5-*c*]quinazolin-8-ylamino)-ethanol 12b

Yield 35% as an off-white solid. ^{1}H NMR (400 MHz, DMSO-d_6) δ 7.84 (d, J = 8.8 Hz, 1H), 7.01 (dd, J = 8.8, 2.3 Hz, 1H), 6.98 (t, J = 0.9 Hz, 1H), 6.83 (d, J = 1.0 Hz, 2H), 6.76 (d, J = 2.2 Hz, 1H), 6.48 (t, J = 5.5 Hz, 1H), 6.21 (s, 2H), 5.96 (s, 2H), 4.75 (t, J = 5.5 Hz, 1H), 4.31 (s, 2H), 3.60 (q, J = 5.8 Hz, 2H), 3.22 (q, J = 5.8 Hz, 2H). LCMS: m/z 379 $[M+H]^+$ at rt 4.5 min; HRMS (ESI) calcd for $C_{19}H_{19}N_6O_3$ $[M+H]^+$ 379.1513 found 379.1513.

5.1.36. 8-*N*-(2-Amino-ethyl)-5-benzo[1,3]dioxol-5-ylmethyl-[1,2,4]triazolo[1,5-*c*]quinazoline-2,8-diamine 12c

Yield 39% as an off-white solid. ^{1}H NMR (400 MHz, DMSO-d_6) δ 7.84 (d, J = 8.8 Hz, 1H), 6.99 (dd, J = 8.8, 2.4 Hz, 1H), 6.97 (d, J = 1.0 Hz, 1H), 6.83 (d, J = 1.0 Hz, 2H), 6.75 (d, J = 2.2 Hz, 1H), 6.50 (t, J = 5.4 Hz, 1H), 6.21 (s, 2H), 5.96 (s, 2H), 4.31 (s, 2H), 3.14 (q, J = 6.3 Hz, 2H), 2.76 (t, J = 6.3 Hz, 2H), 2.09 (br s, 2H). LCMS: m/z 378 $[M+H]^+$ at rt 3.73 min; HRMS (ESI) calcd for $C_{19}H_{20}N_7O_2$ $[M+H]^+$ 378.1673 found 378.1678.

5.1.37. 5-Benzo[1,3]dioxol-5-ylmethyl-*N*-8-(2-dimethylamino-ethyl)-[1,2,4]triazolo[1,5-*c*]quinazoline-2,8-diamine 12d

Yield 33% as an off-white solid. ^{1}H NMR (400 MHz, DMSO-d_6) δ 7.86 (d, J = 8.8 Hz, 1H), 7.03 (dd, J = 8.8, 2.3 Hz, 1H), 6.98 (s, 1H), 6.84 (d, J = 1.0 Hz, 2H), 6.77 (d, J = 2.1 Hz, 1H), 6.37 (t, J = 5.2 Hz, 1H), 6.23 (s, 2H), 5.97 (s, 2H), 4.32 (s, 2H), 3.25 (q J = 4.9 Hz, 2H), 2.57 (t, J = 4.9 Hz, 2H), 2.28 (s, 6H). LCMS: m/z 406 $[M+H]^+$ at rt 3.79 min; HRMS (ESI) calcd for $C_{21}H_{24}N_7O_2$ $[M+H]^+$ 406.1986 found 406.1992.

5.1.38. 5-Benzo[1,3]dioxol-5-ylmethyl-*N*-8-(2-pyrrolidin-1-yl-ethyl)-[1,2,4]triazolo[1,5-*c*]quinazoline-2,8-diamine 12e

Yield 30% as an off-white solid. ^{1}H NMR (400 MHz, DMSO-d_6) δ 7.86 (d, J = 8.7 Hz, 1H), 7.02 (dd, J = 8.8, 2.3 Hz, 1H), 6.98 (s, 1H), 6.84 (d, J = 1.1 Hz, 2H), 6.77 (d, J = 2.0 Hz, 1H), 6.45 (t, J = 5.5 Hz, 1H), 6.23 (s, 2H), 5.97 (s, 2H), 4.32 (s, 2H), 3.25–3.29 (m, 2H), 2.55–2.70 (br m, 6H) 1.74 (br s, 4H). LCMS: m/z 432 $[M+H]^+$ at rt 3.91 min; HRMS (ESI) calcd for $C_{23}H_{26}N_7O_2$ $[M+H]^+$ 432.2143 found 432.2151.

5.1.39. 5-Benzo[1,3]dioxol-5-ylmethyl-8-(4-methyl-piperazin-1-yl)-[1,2,4]triazolo[1,5-*c*]quinazolin-2-ylamine 12f

Yield 50% as an off-white solid. ^{1}H NMR (400 MHz, DMSO-d_6) δ 7.98 (d, J = 9.0 Hz, 1H), 7.39 (dd, J = 9.0, 2.4 Hz, 1H), 7.13 (d, J = 2.4 Hz, 1H), 6.98 (t, J = 1.0 Hz, 1H), 6.83 (d, J = 1.0 Hz, 2H), 6.30 (s, 2H), 5.96 (s, 2H), 4.35 (s, 2H), 3.35 (m, 4H), 2.46 (m, 4H), 2.23 (s, 3H). LCMS: m/z 418 $[M+H]^+$ at rt 3.98 min; HRMS (ESI) calcd for $C_{22}H_{24}N_7O_2$ $[M+H]^+$ 418.1986 found 418.1987.

5.1.40. 5-Benzo[1,3]dioxol-5-ylmethyl-*N*-8-(2-methoxy-ethyl)-[1,2,4]triazolo[1,5-*c*]quinazoline-2,8-diamine 12g

Yield 37% as an off-white solid. ^{1}H NMR (400 MHz, DMSO-d_6) δ 7.85 (d, J = 8.9 Hz, 1H), 7.03 (dd, J = 8.8, 2.3 Hz, 1H), 6.98 (s, 1H), 6.84 (d, J = 1.1 Hz, 2H), 6.77 (d, J = 2.2 Hz, 1H), 6.55 (br s, 1H), 6.23 (br s, 2H), 5.97 (s, 2H), 4.32 (s, 2H), 3.55 (t, J = 5.5 Hz, 2H), 3.33 (m, 2H), 3.30 (s, 3H). LCMS: m/z 393 $[M+H]^+$ at rt 5.2 min; HRMS (ESI) calcd for $C_{20}H_{21}N_6O_3$ $[M+H]^+$ 418.1986 found 418.1987.

5.1.41. 2-Amino-5-(1,3-benzodioxol-5-ylmethyl)-*N*-(2-hydroxyethyl)[1,2,4]triazolo[1,5-*c*]quinazoline-8-carboxamide 13a

To a solution of **7v** (0.05 g, 0.14 mmol), and 2-aminoethanol (0.017 mL, 0.28 mmol) in anhydrous dichloromethane (5 mL), TBTU (0.05 g, 0.17 mmol) was added. The reaction was stirred at room temperature for 30 min, then 2-aminoethanol (0.02 mL, 0.28 mmol) was added. After stirring for 1 h, the solution was washed with $NaHCO_3$ saturated solution, then with water and brine. The organic phase was dried over Na_2SO_4 and evaporated to give a crude that was purified by flash column chromatography on silica gel eluting with DCM/EtOH/NH_4OH 8:1.9:0.1, to provide the title compound (22 mg, 40% yield). ^{1}H NMR (400 MHz, DMSO-d_6) δ 8.74 (t, J = 5.6 Hz, 1H), 8.36 (d, J = 1.4 Hz, 1H), 8.26 (d, J = 8.3 Hz, 1H), 8.16 (br s, 1H), 8.07 (dd, J = 8.3, 1.4 Hz, 1H), 7.01 (d, J = 1.0 Hz, 1H), 6.82–6.92 (m, 2H), 6.54 (s, 2H), 5.98 (s, 2H), 4.73 (t, J = 5.7 Hz, 1H), 4.45 (s, 2H), 3.54 (q, J = 6.1 Hz, 2H), 3.34–3.42 (m, 1H), 1.26 (d, 1H). LCMS: m/z 407 $[M+H]^+$ at rt 4.29 min; HRMS (ESI) calcd for $C_{20}H_{19}N_6O_4$ $[M+H]^+$ 407.1463 found 407.146. The following compound **13b** was prepared according to the method described above.

5.1.42. 2-Amino-5-(1,3-benzodioxol-5-ylmethyl)-*N*-(3-hydroxypropyl)[1,2,4]triazolo[1,5-*c*]quinazoline-8-carboxamide 13b

Yield 30% as an off-white solid. ^{1}H NMR (400 MHz, DMSO-d_6) δ 8.74 (t, J = 5.4 Hz, 1H), 8.34 (d, J = 1.2 Hz, 1H), 8.26 (d, J = 8.4 Hz, 1H), 8.07 (dd, J = 8.4, 1.6 Hz, 1H), 7.01 (d, J = 1.0 Hz, 1H), 6.86 (m, 2H), 6.54 (s, 2H), 5.98 (s, 2H), 4.45 (s, 2H), 4.47 (m, 1H), 3.49 (m, 2H), 3.36 (m, 2H), 1.71 (m, 2H). LCMS: m/z 421 $[M+H]^+$ at rt 4.4 min; HRMS (ESI) calcd for $C_{21}H_{21}N_6O_4$ $[M+H]^+$ 421.1619 found 421.1613.

5.1.43. 2-{[2-Amino-5-(1,3-benzodioxol-5-ylmethyl)[1,2,4]triazolo[1,5-*c*]quinazolin-10-yl]amino}ethanol 14

To 5-benzo[1,3]dioxol-5-ylmethyl-10-fluoro-[1,2,4]triazolo[1,5-*c*]quinazolin-2-ylamine **7o** (0.05 g, 0.15 mmol), 2-aminoethanol (0.7 mL) was added and the mixture was heated at 140 °C for 2–8 h. The reaction was cooled at room temperature, the solid precipitated was filtered and washed with a mixture MeOH/H_2O 9:1, to provide the desired compounds. Yield 60% as a off-white solid. ^{1}H NMR (400 MHz, DMSO-d_6) δ 7.74 (t, J = 5.7 Hz, 1H), 7.53 (t, J = 8.1 Hz, 1H), 6.99 (dd, J = 8.2, 0.6 Hz, 1H), 6.97 (t, J = 1.0 Hz, 1H), 6.82 (d, J = 1.0 Hz, 2H), 6.73 (d, J = 8.2 Hz, 1H), 6.43 (s, 2H), 5.96 (s, 2H), 4.82 (t, J = 5.6 Hz, 1H), 4.37 (s, 2H), 3.66 (q, J = 5.6 Hz, 2H), 3.40 (q, J = 5.9 Hz, 2H). LCMS: m/z 379 $[M+H]^+$ at rt 5.36 min; HRMS (ESI) calcd for $C_{19}H_{19}N_6O_2$ $[M+H]^+$ 379.1513 found 379.1529.

5.1.44. 5-(1,3-Benzodioxol-5-ylmethyl)-10-fluoro-8-(4-methylpiperazin-1-yl)[1,2,4]triazolo[1,5-*c*]quinazolin-2-amine. 17

To a 0–5 °C cooled suspension of **5p** (0.50 g, 1.49 mmol) in dichloromethane (20 mL) was added 2 M (trimethylsilyl)diazomethane diethyl ether solution (0.82 mL, 1.64 mmol). The mixture was stirred at room temperature for 1 h, then the solvent was evaporated, to provide the desired methyl ester (0.52 g, 98% yield). ^{1}H NMR (400 MHz, DMSO-d_6) δ 10.28 (s, 1H), 7.54 (ddd, J = 11.0, 2.4, 1.6 Hz, 1H), 7.15 (ddd, J = 11.1, 8.8, 2.6 Hz, 1H), 6.85–6.93 (m, 2H), 6.68–6.82 (m, 1H), 5.99 (s, 2H), 3.72 (s, 3H), 3.60 (s, 2H). To a solution of 2-(2-benzo[1,3]dioxol-5-yl-acetylamino)-4,6-difluoro-benzoic acid methyl ester (0.50 g, 1.43 mmol) in dimethylsulfoxide (8 mL) was added *N*-methylpiperazine (0.20 mL, 2.86 mmol). The reaction was stirred at 80 °C for 3 h then cooled at room temperature. The precipitated solid was filtered and washed with a mixture H_2O/EtOH 1:1, to provide **15** (0.15 g, 25% yield). ^{1}H NMR (400 MHz, DMSO-d_6) δ 10.52 (s, 1H), 7.58 (d, J = 2.3 Hz, 1H), 6.89 (d, J = 1.6 Hz, 1H), 6.87 (d, J = 7.9 Hz, 1H), 6.78 (dd, J = 7.9, 1.7 Hz, 1H), 6.56 (dd, J = 15.5, 2.4 Hz, 1H), 5.99 (s, 2H), 3.71 (s, 3H), 3.60 (s, 2H), 3.28 (m, 4H), 2.41 (br s, 4H), 2.22 (s, 3H). To a suspension of 2-(2-benzo[1,3]dioxol-5-yl-acetylamino)-6-fluoro-4-(4-methyl-piperazin-1-yl)-benzoic acid methyl ester **15** (0.15 g, 0.35 mmol) in a mixture of tetrahydrofuran (10 mL), methanol (1 mL) and water (2 mL), was added lithium hydroxide (0.15 g, 3.49 mmol). The reaction was stirred at room temperature overnight then the solvent was evaporated. The residue was diluted with water and 2 N HCl solution was added until pH 7. The solid precipitated was filtered and washed with water to obtain crude 2-(2-benzo[1,3]dioxol-5-yl-acetylamino)-6-fluoro-4-(4-methyl-piperazin-1-yl)-benzoic acid. The acid was suspended in acetic anhydride (3 mL) and the reaction mixture was heated under microwave condition at 130 °C for 10 min. The solvent was evaporated to obtain the 2-benzo[1,3]dioxol-5-ylmethyl-5-fluoro-7-(4-methyl-piperazin-1-yl)-benzo[*d*][1,3]oxazin-4-one **16** as crude that was dissolved in dry pyridine (3 mL) then, aminoguanidine hydrogencarbonate (0.05 g, 0.39 mmol) was added and the resulting mixture was heated under microwave condition at 180 °C for 15 min. The reaction was cooled at room temperature and diluted with water to induce the precipitation of a brown solid, which was washed with a mixture MeOH/H_2O 8:2, to afford the title compound (0.07 g, 46% yield). ^{1}H NMR (400 MHz, DMSO-d_6) δ 9.69 (br s, 1H), 7.33 (dd, J = 13.7, 2.2 Hz, 1H), 7.12 (d, J = 2.2 Hz, 1H), 6.97 (m, 1H), 6.81–6.86 (m, 2H), 6.45 (br s, 2H), 5.97 (s, 2H), 4.37 (s, 2H), 4.17 (m, 2H), 3.51 (m, 2H), 3.05–3.23 (m, 4H), 2.86 (s, 3H). LCMS: m/z 436 $[M+H]^+$ at rt

4.08 min; HRMS (ESI) calcd for $C_{22}H_{23}N_7O_4$ $[M+H]^+$ 436.1892 found 436.1891.

5.1.45. General procedure for preparation of compounds 18a–e

To 5-benzo[1,3]dioxol-5-ylmethyl-8,10-difluoro-[1,2,4]triazolo[1,5-*c*]quinazolin-2-ylamine **7s** (0.05 g, 0.14 mmol), amine derivative (0.7 mL) was added and the mixture was heated at 140 °C for 2–8 h. The reaction was cooled at room temperature, the precipitated solid was filtered and washed with a mixture MeOH/H_2O 9:1 to provide the desired compounds.

5.1.46. 2-{[2-Amino-5-(1,3-benzodioxol-5-ylmethyl)-8-fluoro[1,2,4]triazolo[1,5-*c*]quinazolin-10-yl]amino}ethanol 18a

Yield 62% as an off-white solid. ^{1}H NMR (400 MHz, DMSO-d_6) δ ^{1}H 7.99 (td, J = 5.4, 1.6 Hz, 1H), 6.97 (s, 1H), 6.82 (m, 2H), 6.72 (dd, J = 10.3, 2.3 Hz, 1H), 6.59 (dd, J = 12.6, 2.3 Hz, 1H), 6.48 (s, 2H), 5.96 (s, 2H), 4.85 (t, J = 5.4 Hz, 1H), 4.36 (s, 2H), 3.66 (q, J = 5.5 Hz, 2H), 3.40 (q, J = 5.6 Hz, 2H). LCMS: m/z 397 $[M+H]^+$ at rt 5.73 min; HRMS (ESI) calcd for $C_{19}H_{18}N_6O_3$ $[M+H]^+$ 397.1419 found 397.1419.

5.1.47. 3-{[2-Amino-5-(1,3-benzodioxol-5-ylmethyl)-8-fluoro[1,2,4]triazolo[1,5-*c*]quinazolin-10-yl]amino}propan-1-ol 18b

Yield 63% as an off-white solid. ^{1}H NMR (400 MHz, DMSO-d_6) δ 7.86–7.92 (m, 1H), 6.97 (s, 1H), 6.82 (m, 2H), 6.71 (dd, J = 10.3, 2.3 Hz, 1H), 6.55 (dd, J = 12.5, 2.3 Hz, 1H), 6.51 (s, 2H), 5.96 (s, 2H), 4.57 (t, J = 5.1 Hz, 1H), 4.36 (s, 2H), 3.56 (q, J = 6.0 Hz, 2H), 3.38 (q, J = 6.5 Hz, 2H), 1.81 (quin, J = 6.5 Hz, 2H). LCMS: m/z 411 $[M+H]^+$ at rt 5.9 min; HRMS (ESI) calcd for $C_{20}H_{19}FN_6O_3$ $[M+H]^+$ 411.1576 found 411.157.

5.1.48. 5-(1,3-Benzodioxol-5-ylmethyl)-8-fluoro-N-10-(2-methoxyethyl)[1,2,4]triazolo[1,5-*c*]quinazoline-2,10-diamine 18c

Yield 56% as an off-white solid. ^{1}H NMR (400 MHz, DMSO-d_6) δ 7.96 (t, J = 5.4 Hz, 1H), 6.94 (s, 1H), 6.80 (s, 2H), 6.70 (dd, J = 10.4, 2.3 Hz, 1H), 6.59 (dd, J = 12.5, 2.3 Hz, 1H), 6.47 (s, 2H), 5.94 (s, 2H), 4.33 (s, 2H), 3.57 (t, J = 5.2 Hz, 2H), 3.47 (q, J = 5.2 Hz, 2H), 3.29 (s, 3H). LCMS: m/z 411 $[M+H]^+$ at rt 6.56 min; HRMS (ESI) calcd for $C_{20}H_{20}FN_6O_3$ $[M+H]^+$ 411.1576 found 411.1562.

5.1.49. *N*-10-(2-Aminoethyl)-5-(1,3-benzodioxol-5-ylmethyl)-8-fluoro[1,2,4]triazolo[1,5-*c*]quinazoline-2,10-diamine 18d

Yield 67% as an off-white solid. ^{1}H NMR (400 MHz, DMSO-d_6) δ 7.99 (m, 1H), 6.97 (s, 1H), 6.83 (m, 2H), 6.72 (dd, J = 10.3, 2.3 Hz, 1H), 6.60 (dd, J = 12.5, 2.3 Hz, 1H), 6.51 (s, 2H), 5.97 (s, 2H), 4.37 (s, 2H), 3.24–3.35 (m, 2H), 2.84 (t, J = 6.3 Hz, 2H). LCMS: m/z 396 $[M+H]^+$ at rt 4.48 min; HRMS (ESI) calcd for $C_{19}H_{19}FN_7O_2$ $[M+H]^+$ 396.1579 found 396.1582.

5.1.50. 5-(1,3-Benzodioxol-5-ylmethyl)-8-fluoro-10-(4-methylpiperazin-1-yl)[1,2,4]triazolo[1,5-*c*]quinazolin-2-amine 18e

Yield 60% as an off-white solid. ^{1}H NMR (400 MHz, DMSO-d_6) δ 7.18 (dd, J = 9.6, 2.5 Hz, 1H), 7.00 (dd, J = 11.2, 2.5 Hz, 1H), 6.97 (s, 1H), 6.82 (d, J = 0.9 Hz, 2H), 6.33 (s, 2H), 5.96 (s, 2H), 4.39 (s, 2H), 3.09 (br s, 4H), 2.64 (m, 4H), 2.30 (s, 3H). LCMS: m/z 436 $[M+H]^+$ at rt 4.54 min; HRMS (ESI) calcd for $C_{22}H_{23}FN_7O_2$ $[M+H]^+$ 436.1892 found 436.1879.

5.2. NMR FAXS screening method

FAXS (Fluorine chemical shift Anisotropy and eXchange for Screening) method[9] is a NMR binding competition technique that requires the use of a fluorinated reference compound (the so-called 'spy molecule') that binds at the protein active site with medium to low affinity and whose displacement is monitored during the screening of the fragment library. Fluorine NMR experiments were carried out at 564 MHz, using an Inova 600 instrument (Varian, Palo Alto, USA) equipped with a ^{19}F–^{1}H probe and with an autosampler. Samples for NMR screening were prepared in 50 mM Hepes buffer, pH 7.2, containing 100 mM KCl, 5 mM $MgCl_2$, 10 μM EDTA and 8% D_2O. A library of 300 fluorine-containing molecules was initially tested in mixtures (5–10 fluorine fragments in each mixture) against Hsp90 for the identification of potential spy molecules. Mixtures were tested at 50 μM concentration using ^{19}F one dimensional T_2 filter experiments recorded in the absence and presence of 1.5 μM Hsp90. As a result, **1** and **2** were identified as suitable spy molecules. However, compound **2** was selected as the more appropriated for our purpose to identify ATP binding site ligands, as well as alternative site binders. In addition, a molecule that does not interact with the receptor was selected from the library of 300 fluorine (CF and CF_3) compounds and used as control molecule. Titration NMR experiments with the selected fluorinated compound are performed for finding the optimal set-up conditions for the assay and for deriving the binding constants of the identified hits.[9] Typical screening samples against Hsp90 contained 0.016 mg/mL (0.6 μM) Hsp90 α (25,600 Da), 6 μM of the spy molecule (K_D 7.5 μM, value measured using a competition binding FP assay), 6 μM of control molecule, and 50 μM (0.2% DMSO-d_6) of the tested fragments. FAXS experiments were performed using the Carr–Purcell–Meiboom–Gill (CPMG) spin-echo scheme[36] with length of 240 and 480 ms before the acquisition period. Spectra were collected at 293 K using 128 transients. Intensity reduction of the signal of the spy molecule in the presence of the protein due to shortening of its transverse relaxation is a marker of the interactions of the molecule with the protein. Intensity recovery of the signal in the presence of a competitive ligand that displaced the spy molecule is an indication of specific binding.[9] The use of a weak affinity ligand in combination with the competition binding experiments permits rapid ranking of compounds for their binding affinity.[9] For these reasons we used the FAXS method not only to screen the fragment library, but also to follow the SAR during the initial stages of the optimization process.

5.3. Crystallographic methods

Crystallization studies were performed using the *N*-terminal domain of Hsp90α (aa 9-236). Crystals of the apo protein were obtained by vapor diffusion by mixing equal volumes of protein (25 mg/ml in 25 mM TRIS pH 7,6, 150 mM NaCl, 1 mM DTT) and reservoir solutions (20–25% MPEG2000, Cacodylate 0.1 M pH 6.5, 200 mM $MgCl_2$) at 4 °C. Crystals of HSp90 in complex with compound 3 were obtained by soaking. Crystals of the apo protein were transferred to a buffer solution similar to the one used in the NMR assay (0.1 M Hepes pH 7.2, 30% MPEG2000 + 10% of 100 mM stock solution of NMS-00953205 in DMSO) and left to equilibrate overnight at 4 °C before freezing.

Crystals of the *N*-terminal domain of Hsp90 in complex with the other compounds **8b**, **7h**, **7l**, **7o**, **7n**, **12b** and **18a** were obtained by co-crystallization from a solution of 20–25% PEG 3350 K, 0.1 M magnesium chloride, 0.1 M BIS-TRIS pH 5.5–6.5 at 4 °C The protein was concentrated at 25 mg/mL and compound was added to a nominal concentration of 2 mM. For data collection, the crystals were transferred to drops containing the equivalent mother liquor with 25% glycerol. Diffraction data were collected in house using a Rigaku Micromax-007 HF X-ray generator and Mar345 Image Plate Detector (Marresearch). Data were processed using the HKL package.[37] Model building was done using Coot[38] and refinement was done with RefMac.[39] The coordinates have been deposited in the Protein Data Bank with code 4CWF, 4CWN, 4CWO, 4CWP, 4CWQ, 4CWR, 4CWS and 4CWT.

5.4. Molecular modeling

All molecular docking and the generation of binding models were performed starting from reported crystallographic structures using the QXP/FLO program. In docking, typical settings correspond to 2000 Monte Carlo conformational search steps and 10 final poses saved. Polar hydrogen atoms were added and optimized with the available QXP/FLO tools.

5.5. Hsp90 binding assays

A commercially available FITC-Geldanamycin (InvivoGen) was used as probe in a Fluorescence Polarization (FP) assay, after its reduction as described.[40] The limit of sensitivity corresponds to the protein concentration in the assay, which is 5 nM. Values below this limit have to be considered in 'tight binding conditions'.[41]

5.6. FP displacement assay

FP displacement assay for Hsc70-FL was set up using a commercially available probe N^6-(6-amino)hexyl-ATP ATTO-590-ATP (JenaBioScience—Germany).

5.7. In vitro kinase assays

Interrogation for potential kinase inhibitory effects was performed on an internally developed Kinase Selectivity Screening (KSS) panel, designed to represent the overall diversity of the kinome, as described in detail in a recent publication.[32]

The panel includes: Bcr-Abl, ACK1, AKT1, ALK, Aur1, Aur2, BUB1, BRK, CDC7/DBF4, CDK2/CYCA, CHK1, CK2, EEF2K, EGFR1, ERK2, EphA2, FAK, FGFR1, FLT3, GSK3β, Haspin, IGFR1, IKK2, IR, JAK1, JAK2, JAK3, KIT, LCK, LYN, MAPKAPK2, MELK, c-MET, MNK2, MPS1, MST4, NEK6, NIM1, P38α, PAK4, PDGFR, PDK1, PERK, PKAα, PKCβ, PLK1, RET, ROS1, SULU1, Syk, TRKA, TLK2, TYK2, VEGFR2, VGFR3, ZAP70.

5.8. High throughput solubility

Solubility at pH 7 was performed as previously described.[42]

5.9. Cell proliferation assay

Cells were seeded into 96- or 384-wells plates at final concentration ranging from 10,000 to 30,000 cells per cm^2 in appropriate medium plus 10% FCS. After 24 h cells were treated using serial dilution of compounds in two replicates. At 72 h after the treatment the amount of cells were evaluated using the Cell Titer-Glo assay (Promega). Inhibitory activity was evaluated comparing treated versus control data using sigmoidal equation on the Assay Explorer (Symix) program.

5.10. Her2 degradation assay

Her2 degradation cellular activity of Hsp90 inhibitors was assessed by measuring the induced loss of Her2 protein levels in BT474 breast cancer cells. Cellular Her2 levels were measured by immunocytochemistry, and quantified using an ArrayScan vTi instrument (Cellomics Thermo Scientific). IC_{50} values represent the compound concentration at which cellular Her2 signal is diminished by 50% compared with untreated controls.

Acknowledgments

We thank Daniele Donati, Christian Orrenius and Maurizio Pulici, for reviewing the manuscript. We are grateful to the analytical and purification chemistry labs and to the compound management group for compound characterization, purification and handling.

Supplementary data

Supplementary data associated with this article can be found, in the online version, at http://dx.doi.org/10.1016/j.bmc.2014.05.056.

References and notes

1. (a) Workman, P.; Burrows, F.; Neckers, L.; Rosen, N. *Ann. N.Y. Acad. Sci.* **2007**, *1113*, 202; (b) Whitesell, L.; Lindquist, S. *Nat. Rev. Cancer* **2005**, *5*, 761; (c) Neckers, L.; Workman, P. *Clin. Cancer Res.* **2012**, *18*, 64.
2. Picard, D. *Biochim. Biophys. Acta* **2012**, *1823*, 605.
3. Jhaveri, K.; Taldone, T.; Modi, S.; Chiosis, G. *Biochim. Biophys. Acta* **2012**, *1823*, 742.
4. Patel, H. J.; Modi, S.; Chiosis, G.; Taldone, T. *Expert Opin. Drug Discov.* **2011**, *6*, 559.
5. *Fragment-Based Drug Discovery: A Practical Approach*; Zartler, E., Shapiro, M., Eds.; John Wiley and Sons: Hoboken, NJ, 2008; Fragment-Based Drug Design: Tools, Practical Approaches, and Examples In *Methods in Enzymology*; Kuo, L. C., Ed.; Elsevier: San Diego, 2011; Vol. 317,.
6. Roughley, S. D.; Hubbard, R. E. *J. Med. Chem.* **2011**, *54*, 3989.
7. Murray, C. W.; Rees, D. C. *Nat. Chem.* **2009**, *1*, 187.
8. Davis, B. J.; Erlanson, D. A. *Bioorg. Med. Chem. Lett.* **2013**, *13*, 2844.
9. (a) Dalvit, C.; Flocco, M.; Stockman, B. J.; Veronesi, M. *Comb. Chem. High Throughput Screen* **2002**, *5*, 605; (b) Dalvit, C.; Fagerness, P. E.; Hadden, D. T.; Sarver, R. W.; Stockman, B. J. *J. Am. Chem. Soc.* **2003**, *125*, 7696; (c) Dalvit, C. *Prog. Nucl. Magn. Reson. Spectrosc.* **2007**, *51*, 243; (d) Vulpetti, A.; Hommel, U.; Landrum, G.; Lewis, R.; Dalvit, C. *J. Am. Chem. Soc.* **2009**, *131*, 12949.
10. (a) Kim, Y. C.; Ji, X. D.; Jacobson, K. A. *J. Med. Chem.* **1996**, *39*, 4142; (b) Kim, Y. C.; de Zwart, M.; Chang, L.; Moro, S.; von Frijtag Drabbe Künzel, J. K.; Melman, N.; Ijzerman, A. P.; Jacobson, K. A. *J. Med. Chem.* **1998**, *41*, 2835.
11. Kehler, J.; Ritzen, A.; Langgård, M.; Petersen, S. L.; Farah, M. M.; Bundgaard, C.; Christoffersen, C. T.; Nielsen, J.; Kilburn, J. P. *Bioorg. Med. Chem. Lett.* **2011**, *21*, 3738.
12. Westman, J.; Norstedt, G. WO 2005/018532 A2, 2005.
13. Lau, W.; Withka, J., et al. *J. Comput.-Aided Mol. Des.* **2011**, *25*, 621.
14. Morley, A. D.; Pugliese, A.; Birchall, K.; Bower, J.; Brennan, P.; Brown, N.; Chapman, T.; Drysdale, M.; Gilbert, I. H.; Hoelder, S.; Jordan, A.; Ley, S. V.; Merritt, A.; Miller, D.; Swarbrick, M. E.; Wyatt, P. G. *Drug Discovery Today* **2013**, *18*, 1221.
15. Dalvit, C.; Caronni, D.; Mongelli, N.; Veronesi, M.; Vulpetti, A. *Curr. Drug Discov. Technol.* **2006**, *3*, 115.
16. (a) Baell, J. B. *J. Chem. Inf. Model.* **2013**, *53*, 39; (b) Baell, J. B.; Holloway, G. A. *J. Med. Chem.* **2010**, *53*, 2719.
17. (a) Huth, J. R.; Park, C.; Petros, A. M.; Kunzer, A. R.; Wendt, M. D.; Wang, X.; Lynch, C. L.; Mack, J. C.; Swift, K. M.; Judge, R. A.; Chen, J.; Richardson, P. L.; Jin, S.; Tahir, S. K.; Matayoshi, E. D.; Dorwin, S. A.; Ladror, U. S.; Severin, J. M.; Walter, K. A.; Bartley, D. M.; Fesik, S. W.; Elmore, S. W.; Hajduk, P. J. *Chem. Biol. Drug Des.* **2007**, *70*, 1; (b) Murray, C. W.; Carr, M. G.; Callaghan, O.; Chessari, G.; Congreve, M.; Cowan, S.; Coyle, J. E.; Downham, R.; Figueroa, E.; Frederickson, M.; Graham, B.; McMenamin, R.; O'Brien, M. A.; Patel, S.; Phillips, T. R.; Williams, G.; Woodhead, A. J.; Woolford, A. J. A. *J. Med. Chem.* **2010**, *53*, 5942.
18. (a) Brasca, M. G.; Mantegani, S.; Amboldi, N.; Bindi, S.; Caronni, D.; Casale, E.; Ceccarelli, W.; Colombo, N.; De Ponti, A.; Donati, D.; Ermoli, A.; Fachin, G.; Felder, E. R.; Ferguson, R. D.; Fiorelli, C.; Guanci, M.; Isacchi, A.; Pesenti, E.; Polucci, P.; Riceputi, L.; Sola, F.; Visco, C.; Zuccotto, F.; Fogliatto, G. *Bioorg. Med. Chem.* **2013**, *21*, 7047; (b) Fogliatto, G.; Gianellini, L.; Brasca, M. G.; Casale, E.; Ballinari, D.; Ciomei, M.; Degrassi, A.; De Ponti, A.; Germani, M.; Guanci, M.; Paolucci, M.; Polucci, P.; Russo, M.; Sola, F.; Valsasina, B.; Visco, C.; Zuccotto, F.; Donati, D.; Felder, E.; Pesenti, E.; Galvani, A.; Mantegani, S.; Isacchi, A. *Clin. Cancer Res.* **2013**, *19*, 3520.
19. (a) Abad-Zapatero, C.; Metz, J. M. *Drug Discovery Today* **2005**, *10*, 464; (b) Hopkins, A. L.; Keseru, G. M.; Leeson, P. D.; Rees, D. C.; Reynolds, C. H. *Nat. Rev. Drug Disc.* **2014**, *13*, 105.
20. Immormino, R. M.; Kang, Y.; Chiosis, G.; Gewirth, D. T. *J. Med. Chem.* **2006**, *49*, 4953.
21. Vallée, F.; Carrez, C.; Pilorge, F.; Dupuy, A.; Parent, A.; Bertin, L.; Thompson, F.; Ferrari, P.; Fassy, F.; Lamberton, A.; Thomas, A.; Arrebola, R.; Guerif, S.; Rohaut, A.; Certal, V.; Ruxer, J. M.; Gouyon, T.; Delorme, C.; Jouanen, A.; Dumas, J.; Grépin, C.; Combeau, C.; Goulaouic, H.; Dereu, N.; Mikol, V.; Mailliet, P.; Minoux, H. *J. Med. Chem.* **2011**, *54*, 7206.
22. Ried, W.; Valentin, J. *Chem. Ber.* **1968**, *101*, 2106.
23. Detailed experimentals for this manuscript are found in the following patent Casale, E.; Casuscelli, F.; Dalvit, C.; Polucci, P.; Zuccotto, F. [1,2,4]triazolo[1,5-c]pyrimidine derivatives as Hsp90 modulators. WO/2011/029775, 2011.
24. Hennequin, L. F.; Allen, J.; Breed, J.; Curwen, J.; Fennell, M.; Green, T. P.; Lambert-van der Brempt, C.; Morgentin, R. m.; Norman, R. A.; Norman, A.; Norman, L.; Plé, P. A.; Warin, N.; Costello, G. *J. Med. Chem.* **2006**, *49*, 6465.
25. Barker, J. J.; Barker, O.; Courtney, S. M.; Gardiner, M.; Hesterkamp, T.; Ichihara, O.; Mather, O.; Montalbetti, C. A.; Müller, A.; Varasi, M.; Whittaker, M.; Yarnold, C. J. *ChemMedChem* **2010**, *5*, 1697.
26. Cheung, K. M.; Matthews, T. P.; James, K.; Rowlands, M. G.; Boxall, K. J.; Sharp, S. Y.; Maloney, A.; Roe, S. M.; Prodromou, C.; Pearl, L. H.; Aherne, G. W.; McDonald, E.; Workman, P. *Bioorg. Med. Chem. Lett.* **2005**, *15*, 3338.

27. Brough, P. A.; Aherne, W.; Barril, X.; Borgognoni, J.; Boxall, K.; Cansfield, J. E.; Cheung, K. M.; Collins, I.; Davies, N. G.; Drysdale, M. J.; Dymock, B.; Eccles, S. A.; Finch, H.; Fink, A.; Hayes, A.; Howes, R.; Hubbard, R. E.; James, K.; Jordan, A. M.; Lockie, A.; Martins, V.; Massey, A.; Matthews, T. P.; McDonald, E.; Northfield, C. J.; Pearl, L. H.; Prodromou, C.; Ray, S.; Raynaud, F. I.; Roughley, S. D.; Sharp, S. Y.; Surgenor, A.; Walmsley, D. L.; Webb, P.; Wood, M.; Workman, P.; Wright, L. *J. Med. Chem.* **2008**, *51*, 196.
28. (a) Chiosis, G.; Lucas, B.; Shtil, A.; Huezo, H.; Rosen, N. *Bioorg. Med. Chem.* **2002**, *10*, 55; (b) Wright, L.; Barril, X.; Dymock, B.; Sheridan, L.; Surgenor, A.; Beswick, M.; Drysdale, M.; Collier, A.; Massey, A.; Davies, N.; Fink, A.; Fromont, C.; Aherne, W.; Boxall, K.; Sharp, S.; Workman, P.; Hubbard, R. E. *Chem. Biol.* **2004**, *11*, 775.
29. (a) Taldone, T.; Chiosis, G. *Curr. Top. Med. Chem.* **2009**, *9*, 1436; (b) Caldas-Lopes, E.; Cerchietti, L.; Ahn, J. H.; Clement, C. C.; Robles, A. I.; Rodina, A.; Moulick, K.; Taldone, T.; Gozman, A.; Guo, Y.; Wu, N.; de Stanchina, E.; White, J.; Gross, S. S.; Ma, Y.; Varticovski, L.; Melnick, A.; Chiosis, G. *Proc. Natl. Acad. Sci. U.S.A.* **2009**, *106*, 8368.
30. Brough, P. A.; Barril, X.; Borgognoni, J.; Chene, P.; Davies, N. G. M.; Davis, B.; Drysdale, M. J.; Dymock, B.; Eccles, S. A.; Garcia-Echeverria, C.; Fromont, C.; Hayes, A.; Hubbard, R. E.; Jordan, A. M.; Jensen, M. R.; Massey, A.; Merrett, A.; Padfield, A.; Parsons, R.; Radimerski, T.; Raynaud, F. I.; Robertson, A.; Roughley, S. D.; Schoepfer, J.; Simmonite, H.; Sharp, S. Y.; Surgenor, A.; Valenti, M.; Walls, S.; Webb, P.; Wood, M.; Workman, P.; Wright, L. *J. Med. Chem.* **2009**, *52*, 4794.
31. Dymock, B.; Barril, X.; Beswick, M.; Collier, A.; Davies, N.; Drysdale, M.; Fink, A.; Fromont, C.; Hubbard, R. E.; Massey, A.; Surgenor, A.; Wright, L. *Bioorg. Med. Chem. Lett.* **2004**, *14*, 325.
32. Felder, E. R.; Badari, A.; Disingrini, T.; Mantegani, S.; Orrenius, C.; Avanzi, N.; Isacchi, A.; Salom, B. *Mol. Diversity* **2012**, *16*, 27.
33. Caco-2 permeability assay, metabolic stability assay with liver microsomes and hepatocytes, CYP inhibition, hERG inhibition assay, and PK studies were carried out at Accelera (www.accelera.org).
34. Rizzo, V.; Pinciroli, V. *J. Pharm. Biomed. Anal.* **2005**, *38*, 851.
35. Colombo, M.; Riccardi-Sirtori, F.; Rizzo, V. *Rapid Commun. Mass Spectrom.* **2004**, *18*, 511.
36. (a) Carr, H. Y.; Purcell, E. M. *Phys. Rev.* **1954**, *94*, 630; (b) Meiboom, S.; Gill, D. *Rev. Sci. Instrum.* **1958**, *29*, 688.
37. Otwinowski, Z.; Minor, W. *Methods Enzymol.* **1997**, *276*, 307.
38. Emsley, P.; Cowtan, K. *Acta Crystallogr. D Biol. Crystallogr.* **2004**, *60*, 2126.
39. Murshudov, G. N.; Vagin, A. A.; Dodson, E. J. *Acta Crystallogr. D Biol. Crystallogr.* **1997**, *53*, 240.
40. Lundgren, K.; Zhang, H.; Brekken, J.; Huser, N.; Powell, R. E.; Timple, N.; Busch, D. J.; Neely, L.; Sensintaffar, J. L.; Yang, Y. C.; McKenzie, A.; Friedman, J.; Scannevin, R.; Kamal, A.; Hong, K.; Kasibhatla, S. R.; Boehm, M. F.; Burrows, F. *Mol. Cancer Ther.* **2009**, *8*, 921.
41. Huang, Xinyi. *J. Biomol. Screen.* **2003**, *1*, 34.
42. Pevarello, P.; Brasca, M. G.; Amici, R.; Orsini, P.; Traquandi, G.; Corti, L.; Piutti, C.; Sansonna, P.; Villa, M.; Pierce, B. S.; Pulici, M.; Giordano, P.; Martina, K.; Fritzen, E. L.; Nugent, R. A.; Casale, E.; Cameron, A.; Ciomei, M.; Roletto, F.; Isacchi, A.; Fogliatto, G.; Pesenti, E.; Pastori, W.; Marsiglio, A.; Leach, K. L.; Clare, P. M.; Fiorentini, F.; Varasi, M.; Vulpetti, A.; Warpehoski, M. A. *J. Med. Chem.* **2004**, *47*, 3367.